



Quantifying space-time dynamics of flood event types

Alberto Viglione^{a,*}, Giovanni Battista Chirico^b, Jürgen Komma^a, Ross Woods^c, Marco Borga^d, Günter Blöschl^a

^a Institut für Wasserbau und Ingenieurhydrologie, Technische Universität Wien, Vienna, Austria

^b Dipartimento di Ingegneria Agraria, Università di Napoli Federico II, Naples, Italy

^c National Institute for Water and Atmospheric Research (NIWA), Christchurch, New Zealand

^d Dipartimento Territorio e Sistemi Agro-Forestali, Università degli Studi di Padova, Padua, Italy

ARTICLE INFO

Keywords:

Flood typology
Storm movement
Catchment response
Correlation
Runoff generation
Runoff coefficient

SUMMARY

A generalised framework of space-time variability in flood response is used to characterise five flood events of different type in the Kamp area in Austria: one long-rain event, two short-rain events, one rain-on-snow event and one snowmelt event. Specifically, the framework quantifies the contributions of the space-time variability of rainfall/snowmelt, runoff coefficient, hillslope and channel routing to the flood runoff volume and the delay and spread of the resulting hydrograph. The results indicate that the components obtained by the framework clearly reflect the individual processes which characterise the event types. For the short-rain events, temporal, spatial and movement components can all be important in runoff generation and routing, which would be expected because of their local nature in time and, particularly, in space. For the long-rain event, the temporal components tend to be more important for runoff generation, because of the more uniform spatial coverage of rainfall, while for routing the spatial distribution of the produced runoff, which is not uniform, is also important. For the rain-on-snow and snowmelt events, the spatio-temporal variability terms typically do not play much role in runoff generation and the spread of the hydrograph is mainly due to the duration of the event. As an outcome of the framework, a dimensionless response number is proposed that represents the joint effect of runoff coefficient and hydrograph peakedness and captures the absolute magnitudes of the observed flood peaks.

© 2010 Elsevier B.V. All rights reserved.

1. Introduction

Floods can be generated by a range of different processes, like channel processes (i.e., ice jams, dam breaks, ...), coastal processes (i.e., storminess, high sea levels, ...) or catchment processes (i.e., intense rainfall, snowmelt, catchment saturation, ...). In this paper we focus on the latter class of processes. Floods at different space-time scales can occur during significantly different hydro-meteorological events, depending on the catchment state and the intensity and space-time structure of the hydro-meteorological forcing. The response of a catchment to a given precipitation input is the consequence of the dominant processes influencing runoff genesis within the catchment, according to the dominant catchment state and hydro-meteorological event type (Hirschboeck et al., 2000; Merz and Blöschl, 2003; Parajka, 2010). Moreover, catchment response can change from event to the other as consequence of the different space-time structure of the hydrometeorological forcing within the catchment (Saulnier and Le Lay, 2009; Borga et al., 2007). Recognising the evolution of the catchment behaviour as

well as the effect of different event characteristics for flood generation is important for developing effective flood hazard real-time prediction systems (Norbiato et al., 2008). It is in fact useful for both developing parsimonious and effective flood forecasting models as well as for identifying what source of quantitative precipitation forecast or real time precipitation monitoring are really required (Borga et al., 2008). In a regional study, Merz and Blöschl (2003) analysed a huge number of flood events in Austria, defined flood event types, and classified them. Their aim was to improve the at-site and regional estimation of flood probabilities by stratifying floods by process typology. In order to explore the effects of different event types and catchment state on flood generation, a spatially distributed approach for catchment modelling is required. However, a simple direct comparison of model results for different event types and antecedent catchment conditions would provide just some qualitative indications about the flood response dynamics.

In this study we use the analytical framework presented in Viglione et al. (2010) to express the response of the catchment to different extreme events by mean of quantitative indices of clear physical meaning. The framework allows to assess how the different space-time structure of the precipitation patterns with respect

* Corresponding author. Tel.: +43 1 58801 22317.

E-mail address: viglione@hydro.tuwien.ac.at (A. Viglione).

to the space-time structure of the contributing areas and the spatial organisation of the lateral flow paths, affects the main statistics of the flood response. We characterize flood response with three quantities: (i) the storm-averaged value (i.e., storm rainfall excess), (ii) the mean runoff time (i.e., the time of the centre of mass of the runoff hydrograph at a catchment outlet), and (iii) the variance of the timing of runoff (i.e., the temporal dispersion of the runoff hydrograph). Each of the three catchment response characteristics is disaggregated in two classes of components: the first explained by the catchment average values, the second explained by the spatial and temporal variability of the key variables. This second class of components is expressed by a set of spatial and temporal covariances.

The characterisation of complex physical behaviour by simple indices is needed for the so called *comparative hydrology* in which consistent methods are sought for assessing and quantifying hydrological similarity across a wide range of catchments, events and models (McDonnell and Woods, 2004; Blöschl, 2006). In this context, the components obtained using the framework can be combined into dimensionless numbers to be used in dimensional analysis. Dimensional techniques have been responsible for some of the great advances in hydraulics (Fischer et al., 1979), and start to be used also in catchment hydrology (e.g., Dooge, 1986; Sivapalan et al., 1987; Larsen et al., 1994; Robinson and Sivapalan, 1995; Blöschl and Sivapalan, 1995; Western et al., 1999; Aryal et al., 2002; Atkinson et al., 2002; Farmer et al., 2003; Wagener et al., 2007). Dimensional techniques are powerful for dealing with complex physical problems, since they can potentially describe these systems by very simple relationships. They can be used to define similarity relationships (in this case between flood events) in the same fashion as the Froude and Reynolds numbers have been used in hydraulics (see Wagener et al., 2007, for a review). In this paper, we propose a dimensionless number which represents the joint effect of runoff coefficient and hydrograph peakedness in determining the flood peak.

We study different events occurred in four catchments of the Kamp region, in northern Austria, whose areas range from 77 to 622 km². The aim of the paper is to measure the contribution of the different mechanisms of flow response for different event types. A total of five events are analysed, which are characterised by different spatio-temporal extent and evolution of precipitation, as well as different conditions for the runoff generation. The flood process types follow the classification suggested by Merz and Blöschl (2003): long-rain floods, short-rain floods, flash-floods, rain-on-snow floods and snowmelt floods. Liquid precipitation has been obtained by interpolation of rain-gauges data on a 1 km × 1 km grid and at 15 min time scale. For the more recent events radar data have been used to refine the spatial evolution of the events. For snowmelt and runoff generation (i.e., runoff coefficient), we exploit the outcomes of the Kamp-model, which is currently used in the forecasting system for the Kamp catchment (Reszler et al., 2006; Blöschl et al., 2008). We account for spatial variability of the hillslope routing time throughout the catchment, assuming that each cell responds as a linear reservoir with spatially varying response time (which, however, we assume constant in time). The spatial distribution of the hillslope response time is related to landuse and is consistent with the Kamp model cell response. Regarding the channel routing, we assume that the streams are spread over the entire catchments (every cell is crossed by a stream) and that the stream velocity is constant in time and space, which has been shown to be reasonable for flood routing purposes (Pilgrim, 1976; Beven, 1979). This velocity corresponds to the celerity of a flood wave in a stream network. Following Rinaldo et al. (1991), we also assume that geomorphological dispersion (caused by the distribution of travel distances in a channel network) dominates the effects of hydrodynamic dispersion, which

we neglect. These assumptions are substantial simplifications of reality, which are common to the majority of the models applied for simulating catchment response to storm events and meet our immediate objective, which is to produce insights into the complex interactions among the key variables affecting the flood response. It is important to note that the framework is not intended to be a predictive model but a tool that can quantify the relative importance of the processes involved in flood response and the space-time interactions between rainfall and catchment state during flood events.

In this paper, we first describe our case study catchment and the detailed hydrological model used to retrieve space-time catchment response of five events, then summarise the analytical framework to interpret space-time variability of flood event response, and finally show and discuss the results of applying the framework.

2. Case study

2.1. The Kamp catchment

The Kamp area is located in northern Austria, approximately 120 km north-west of Vienna (see Fig. 1). We consider four catchments: Kamp at Zwettl, Großer Kamp at Neustift, Purzelkamp at Rastenberg and Taffa at Frauenhofen. At the Zwettl stream gauge the catchment size is 622 km² and elevations range from 500 to 1000 m a.s.l. The higher parts of the catchment in the southwest are hilly with deeply incised channels. Towards the catchment outlet in the northeast the terrain is flatter and swampy areas exist along the streams. Typical flow travel times in the river system range from 2 to 4 h. The geology of the catchment is mainly granite and gneiss. Weathering has produced sandy soils with a large storage capacity throughout the catchment. Fifty percent of the catchment is forested. Mean annual precipitation is about 900 mm of which about 300 mm becomes runoff (Parajka et al., 2005). The mean of the maximum annual peak discharges is about 65 m³/s. During moderate flood events, only a small proportion of rainfall contributes to runoff and event runoff coefficients are 10% or less (Merz and Blöschl, 2005). As rainfall increases in magnitude, the runoff response characteristics change fundamentally because of the soil moisture changes in the catchment and the runoff coefficients can exceed 50%. The catchment is hence highly non-linear in its rainfall–runoff response. Representing catchment soil moisture well is hence of utmost importance for producing accurate flood forecasts.

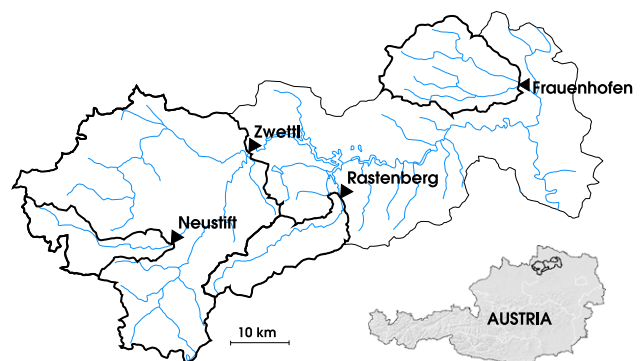


Fig. 1. The Kamp catchment in the northern part of Austria. The four sub-catchments are shown: Kamp at Zwettl, Großer Kamp at Neustift, Purzelkamp at Rastenberg and Taffa at Frauenhofen.

The Neustift catchment has an area of 77 km² and is located in the western-upper part of the Zwettl catchment. The Rastenberg catchment has an area of 95 km², is located south to the Zwettl catchment and has an elongated shape along the Purzelkamp stream (see Fig. 1). The elevation ranges from 500 to 900 m a.s.l. and the geology is dominated by weathered granite. The mean of the maximum annual peak discharges is about 15 m³/s at Neustift and about 11 m³/s at Rastenberg. The same considerations made for the Kamp at Zwettl apply to the Großer Kamp at Neustift and the Purzelkamp at Rastenberg. The Taffa catchment at Frauenhofen is instead different. It is situated in the north-eastern part of the Kamp area and has an area of 140 km². The elevation ranges from 300 to 600 m a.s.l., which is lower than for the other three catchments, and the geology is dominated by gneiss. Mean annual precipitation is also lower, being about 600 mm, and the mean of the maximum annual peak discharges is about 13 m³/s. In the flat, lower part of the Frauenhofen catchment the groundwater system (i.e., the Horner Becken system) controls the hydrologic behavior, intercepting almost all the rainfall and determining very low runoff response.

2.2. The events

Five events which affected the Kamp area are analysed. In Fig. 2 the spatial and temporal evolution of rainfall (and snowmelt) are shown along with the measured discharges at the gauges, when available.

The first event occurred in August 2002 and was a long-rain event (first row in Fig. 2). The rainfall was a frontal type storm and covered a large area including the Kamp catchment. The spatial pattern of the rainfall was quite uniform over the entire catchment. The Vb-cyclone (Mudelsee et al., 2004) is the typical meteorological situation for long-rain events in the region, which was the case in August 2002. In Austria some of the most extreme floods on record have been of this type (Gutknecht et al., 2002) and, in particular, the 2002 event at Zwettl resulted in a peak flow of 460 m³/s which is three times the second largest flood on record (Reszler et al., 2008; Merz and Blöschl, 2008a; Merz and Blöschl, 2008b). The 2002 storm event was composed of two parts of which we analyse here the first one, whose duration was 42 h. Because of the wet period preceding it, the catchment was saturated with high flow conditions. This is typical of long-rain events in which the storage capacity of the catchment is exceeded and any additional rain generates runoff.

The second and third events are short-rain events (second and third rows in Fig. 2). Rainfall of short duration and high intensity (thunderstorms) occurred and saturated parts of the catchments. The volumes of the storm events were moderate (less than 50 mm of rainfall averaged over the catchments occurred) and so were the magnitudes of the floods, which in Zwettl were of the order of 10 m³/s. Quickly moving storm fronts during the summer months are typical meteorological situations for this type of event. Flood runoff resulted from a combination of runoff from saturated areas, runoff from parts of the catchment where the rainfall intensities exceeded infiltration capacity and from fast subsurface flow. In the classification scheme of Merz and Blöschl (2003), both events could be considered as flash-floods, given the short duration and the local spatial extent. Flash-floods are given by short, high intensity rainfalls, mainly of convective origin, which can trigger floods even if the catchment is in a relatively dry condition because, locally, the rainfall intensities exceed infiltration capacity. However, the magnitude of the peaks of these two events is much smaller than that of the long-rain event in 2002.

The fourth and fifth events are characterised by much longer temporal scales and by the presence of snow. The event of April 2006 was a rain-on-snow event (fourth row in Fig. 2). Rain was fall-

ing on an existing snow cover contributing to enhanced snowmelt. Moderate rainfall depths caused considerable runoff depths as a result of a number of mechanisms. During the rainfall, significant long wave radiation and latent heated inputs enhanced snowmelt as compared to dry spells. Antecedent snowmelt saturated large parts of the catchment facilitating overland flow once rain started. The resulting flood peak in Zwettl was quite considerable: 112 m³/s. The event of April 1996 (fifth row in Fig. 2) was a snowmelt event. It occurred during a fair weather period associated with a rapid increase in air temperature. In this type of events, the melt energy is mainly global radiation in higher altitudes and turbulent heat exchange in lower altitudes. Snowmelt occurred over a period of one week, saturating the soils, continuously raising the flows and finally causing a flood. The event was dominated by high baseflow components. Rainfall also occurred but was of minor importance. As there is an upper limit of energy available for melt, these kind of floods are never very extreme. In April 1996 the peak measured in Zwettl was 35 m³/s.

2.3. The Kamp model

To retrieve the detailed spatio-temporal evolution of the runoff coefficient and of snowmelt over the catchments, we use a spatially distributed continuous rainfall–runoff model (Reszler et al., 2006; Blöschl et al., 2008) developed for the Kamp catchment, which is similar to the HBV model (Bergström, 1976). The model runs on a 1 km × 1 km grid and a 15 min time step and consists of a snow routine, a soil moisture routine and a flow routing routine. The snow routine represents snow accumulation and melt by the degree-day concept. The soil moisture routine represents runoff generation and changes in the soil moisture state of the catchment and involves three parameters: the maximum soil moisture storage, a parameter representing the soil moisture state above which evaporation is at its potential rate, termed the limit for potential evaporation, and a parameter in the non-linear function relating runoff generation to the soil moisture state, termed the non-linearity parameter. The details of the soil moisture routine are given in Komma et al. (2008).

Runoff routing on the hillslopes is represented by an upper and two lower soil reservoirs. Excess rainfall enters the upper zone reservoir and leaves this reservoir through three paths: outflow from the reservoir based on a fast storage coefficient; percolation to the lower zones with a percolation rate; and, if a threshold of the storage state is exceeded, through an additional outlet based on a very fast storage coefficient. Water leaves the lower zones based on the slow storage coefficients. Bypass flow is accounted for by recharging the lower zone reservoir directly by a fraction of the excess rainfall. The outflow from the reservoirs represents the total runoff on the hillslope scale. The model states for each grid element are the snow water equivalent, the soil moisture of the top soil layer and the storage of the soil reservoirs associated with the storage coefficients.

The model parameters for each grid element were identified based on the “dominant processes concept” of Grayson and Blöschl (2000) which suggests that, at different locations and different points in time, a small number of processes will dominate over the rest. Land use, soil type, landscape morphology (e.g., the degree of incision of streams) and information on soil moisture and water logging based on field surveys were used. Discussions with locals provided information on flow pathways during past floods. Runoff simulations, stratified by time scale and hydrological situations, were then compared with runoff data, and the simulated subsurface dynamics were compared with piezometric head data. The various pieces of information were finally combined in an iterative way to construct a coherent picture of the functioning of the catchment system, on the basis of which plausible parameters for each

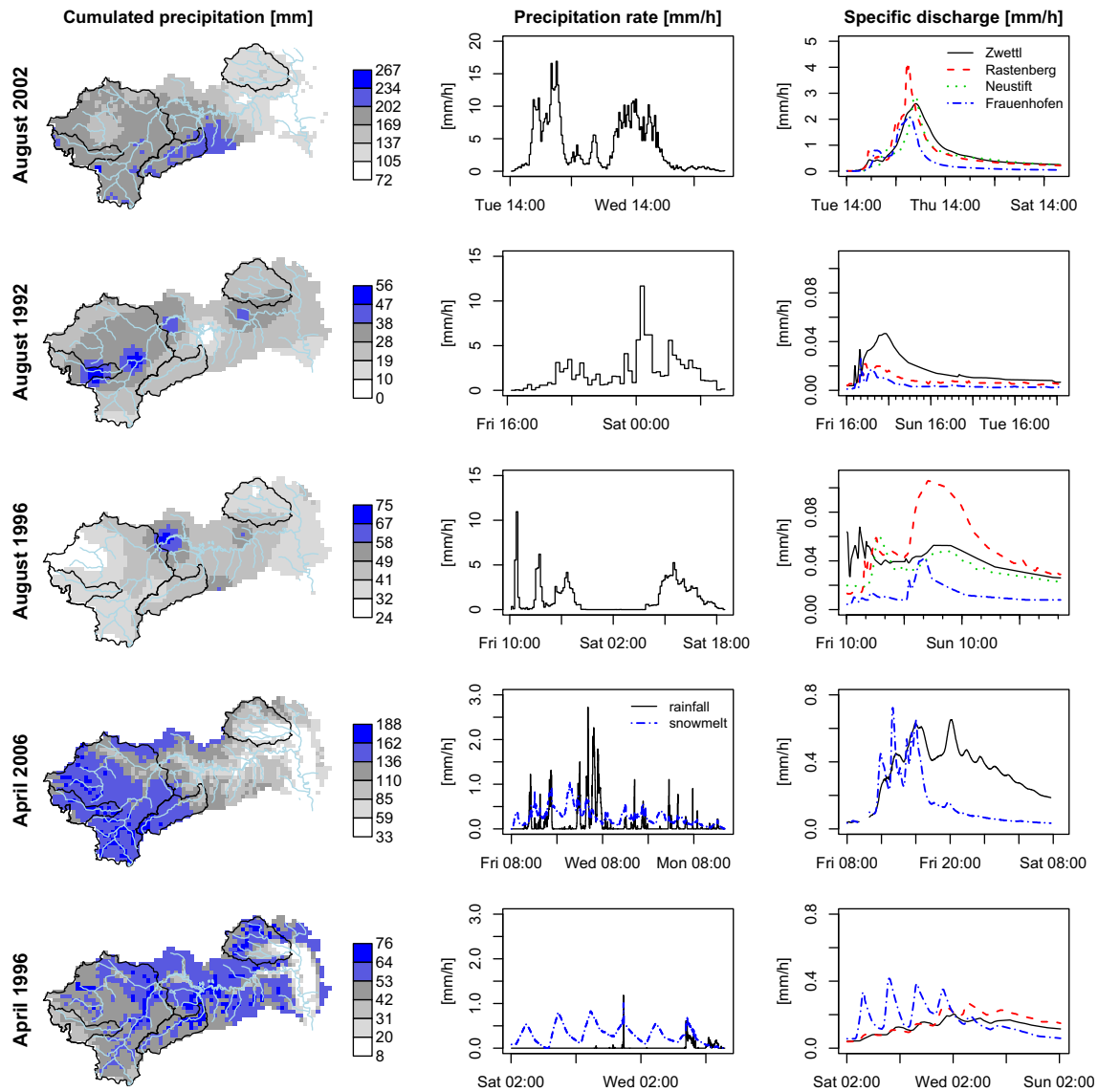


Fig. 2. Measured rainfall/snowmelt and discharge for the five events analysed (showed per row): the long-rain event of August 2002; the short-rain event of August 1992; the short-rain event of August 1996; the rain-on-snow event of April 2006 and the snowmelt event of April 1996. The left column shows the cumulative precipitation (rainfall + snowmelt) on the Kamp region, the central column shows the spatial averaged precipitation rate on the Kamp region and the right column shows the measured discharges at the basins outlets, where available.

grid element were chosen. The model was extensively tested against independent runoff data both at the seasonal and event scales (Blöschl et al., 2008).

The time and space dependent runoff coefficients used in our analyses have been estimated as follows. A first estimate of the runoff coefficient at a grid cell (x, y) and at time t is obtained as $W_0(x, y, t) = (S_s(x, y, t) / L_s(x, y))^{\beta(x, y)}$ where $S_s(x, y, t)$ is the soil moisture [mm] estimated by the model, $L_s(x, y)$ is the maximum soil moisture storage [mm] and $\beta(x, y)$ is the non-linearity parameter []. Since $W_0(x, y, t)$ refers to both fast and slow components of runoff response, $W_0(x, y, t)$ is rescaled in order to account for the fast runoff components only, i.e., $W(x, y, t) = r_f(x, y) \cdot W_0(x, y, t)$. The scaling factor $r_f(x, y)$ is given by the cumulative cell outflow during the flood event divided by the amount of water that enters the cell during the precipitation (and/or snowmelt) event. In this way, the baseflow component of the response is not considered. This is consistent with the framework used here, which focuses on quick flood response only.

3. Analytical framework

In Viglione et al. (2010) we extended the analytical framework developed in Woods and Sivapalan (1999) to characterise flood response in the case where complex space and time variability of both rainfall and runoff generation are considered as well as hillslope and channel network routing. We characterize flood response with three quantities: (i) its storm-averaged value (i.e., catchment rainfall excess), (ii) the mean runoff time (i.e., the time of the center of mass of the runoff hydrograph at a catchment outlet), and (iii) the variance of the timing of runoff (i.e., the temporal dispersion of the runoff hydrograph). The mean time of catchment runoff is a surrogate for the time to peak. The storm-averaged rainfall excess rate and the variance of runoff time, taken together, are indicative of the magnitude of the peak runoff, i.e., for a given event duration and volume of runoff, a sharply peaked hydrograph will have a relatively low variance compared to a more gradually varying hydrograph (see Woods, 1997, for details). The analytical

results obtained in Viglione et al. (2010) are briefly summarised below and illustrated by examples from the above introduced flood events.

3.1. Catchment rainfall excess

We define the rainfall excess $R(x,y,t)$ [LT^{-1}] at a point (x,y) and at time t as follows:

$$R(x,y,t) = P(x,y,t) \cdot W(x,y,t) \quad (1)$$

where $P(x,y,t)$ [LT^{-1}] is the local rainfall and $W(x,y,t)$ [] is the local runoff coefficient, bounded between 0 and 1.

3.1.1. Instantaneous catchment rainfall excess

For a catchment with area A , the instantaneous catchment-averaged rainfall excess rate $R_{x,y}(t)$ [LT^{-1}] at time t can be expressed in terms of the moments of rainfall P and runoff coefficient W by averaging Eq. (1) over the catchment:

$$R_{x,y}(t) = P_{x,y}(t) \cdot W_{x,y}(t) + cov_{x,y}(P, W) \quad (2)$$

where $P_{x,y}(t)$ is the time series of catchment-averaged rainfall rates [LT^{-1}], $W_{x,y}(t)$ is the time series of catchment-averaged runoff coefficient [], and $cov_{x,y}(P, W)$ is the time series of the spatial covariance [LT^{-1}] of P and W . In Fig. 3 the terms of Eq. (2) are shown for the short-rain event of August 1996 on the Kamp catchment at Zwettl. In the top panel the instantaneous catchment-averaged rainfall excess $R_{x,y}(t)$ is compared to the catchment-averaged rainfall $P_{x,y}(t)$. The temporal evolution of the catchment-averaged runoff coefficient $W_{x,y}(t)$ is also displayed. In the bottom panel the effect of spatial correlation between rainfall and runoff generation is shown by comparing $R_{x,y}(t)$ and $P_{x,y}(t) \cdot W_{x,y}(t)$. The difference between them is $cov_{x,y}(P, W)$, which is also shown in the figure. This term is particularly relevant at the beginning of the event (the first two rain

bursts) meaning that, at the beginning of the event, it rains more where the runoff coefficient is high, i.e., in the wet part of the catchment. In the second part of the event, on the contrary, the effect of $cov_{x,y}(P, W)$ is minimal.

3.1.2. Storm-averaged rainfall excess

While Eq. (2) lumps the spatial information and shows the temporal evolution of the rainfall excess, a different view can be obtained averaging Eq. (1) over time. The time-averaged rainfall excess $R_t(x,y)$ [LT^{-1}] for the period $[0, T_m]$ (where T_m is the storm duration) can be expressed in terms of the moments of rainfall P and runoff coefficient W as

$$R_t(x,y) = P_t(x,y) \cdot W_t(x,y) + cov_t(P, W) \quad (3)$$

where $P_t(x,y)$ is the map of the temporally averaged rainfall rates [LT^{-1}], $W_t(x,y)$ is the map of the temporally averaged runoff coefficients [], and $cov_t(P, W)$ is the map of the temporal covariances [LT^{-1}] of P and W . This covariance term is not a constant but varies in space as shown in Fig. 4. Here the same event of August 1996 of Fig. 3 is shown. The rainfall $P_t(x,y)$ is concentrated, on average, close to the catchment outlet where also the runoff coefficient $W_t(x,y)$ is, on average, high. The temporal covariance $cov_t(P, W)$ shown in Fig. 4 is significantly negative close to the outlet. This means that, close to the outlet, it rains more when the runoff coefficient is low, i.e., at the beginning of the event.

3.1.3. Storm-averaged catchment rainfall excess

The storm-averaged catchment rainfall excess $R_{x,y,t}$ [LT^{-1}] is derived by averaging Eq. (2) in time or Eq. (3) in space and can be expressed in terms of the moments of rainfall P and runoff coefficient W as (see Viglione et al., 2010)

$$R_{x,y,t} = \underbrace{P_{x,y,t} \cdot W_{x,y,t}}_{R1} + \underbrace{cov_t(P_{x,y}, W_{x,y})}_{R2} + \underbrace{cov_{x,y}(P_t, W_t)}_{R3} + \underbrace{[cov_t(P - P_{x,y}, W - W_{x,y})]_{x,y}}_{R4} \quad (4)$$

Four statistics of the rainfall and runoff generation fields influence the storm runoff from a catchment:

- (R1) the product of time- and catchment-averaged values of P and W [LT^{-1}];
- (R2) the temporal covariance of the space-averaged P and W [LT^{-1}];
- (R3) the spatial covariance of the time-averaged P and W [LT^{-1}];
- (R4) the spatial variation in temporal covariance (or, equivalently, the temporal variation in spatial covariance) [LT^{-1}].

The term R2 is a measure of the temporal correlation of rainfall and runoff coefficient, which, unlike the term $cov_t(P, W)$ in Eq. (3), ignores their spatial patterns. Analogously, the term R3 measures the spatial correlation of rainfall and runoff coefficient but, unlike the term $cov_{x,y}(P, W)$ in Eq. (2), ignores the temporal evolution of the patterns. The spatio-temporal variabilities not accounted for by terms R2 and R3 are embedded in the term labelled R4. The effect of the movement of P and W on the storm-averaged catchment rainfall excess can be isolated as $R4 - R2 - R3/R1$ (see Viglione et al., 2010). If one considers again the event of August 1996 at Zwettl, the values of each term in Eq. (4) are shown in Table 1 and discussed in the result section.

3.2. Catchment runoff time

Having estimated in Eqs. (2)–(4) the roles of space and time variability of rainfall and runoff generation in controlling rainfall excess, we now examine the influence of hillslope and channel

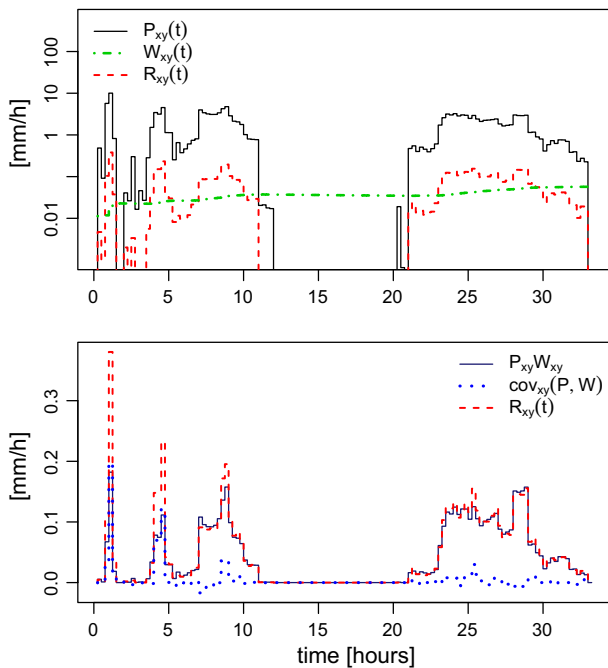


Fig. 3. Instantaneous catchment rainfall excess $R_{x,y}(t)$ and components of Eq. (2). The short-rain event of August 1996 in Zwettl is shown. The top panel shows, in log-scale: the time series of the catchment-averaged rainfall rate $P_{x,y}(t)$; the time series of the catchment-averaged runoff coefficient $W_{x,y}(t)$; and the time series of the catchment-averaged rainfall excess rate $R_{x,y}(t)$. The bottom panel shows: the time series of the product $P_{x,y}(t) \cdot W_{x,y}(t)$; the time series of the spatial covariance $cov_{x,y}(P, W)$ between $P(x,y,t)$ and $W(x,y,t)$; and the time series of the catchment-averaged rainfall excess rate $R_{x,y}(t)$.

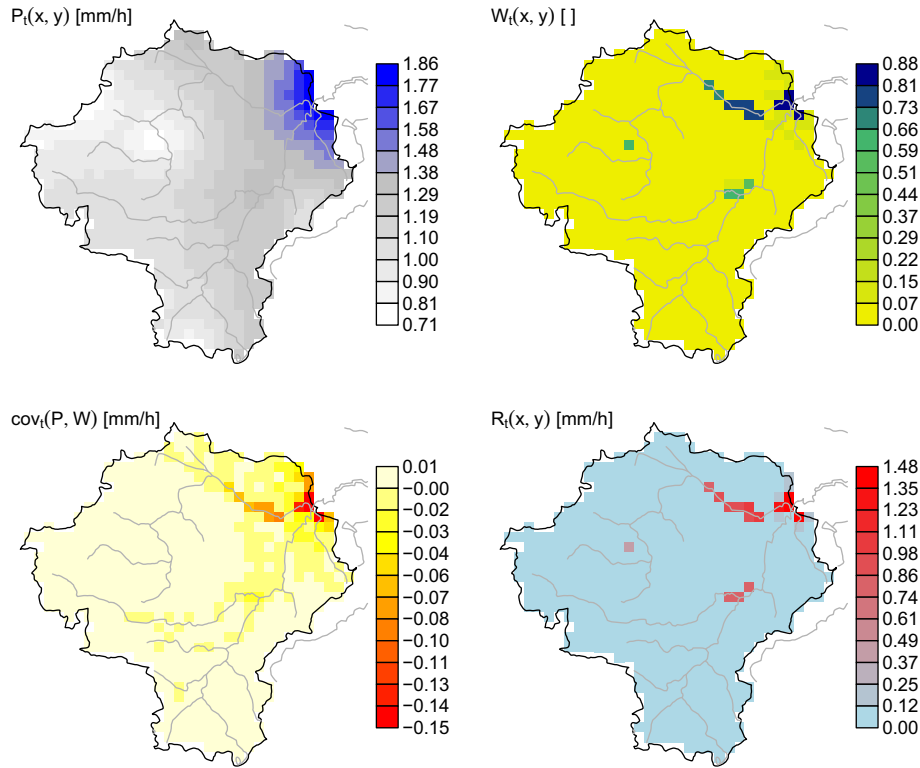


Fig. 4. Storm-averaged rainfall excess $R_t(x,y)$ and components of Eq. (3). The short-rain event of August 1996 in Zwettl is shown. Proceeding for rows, the figure shows: the map of the temporally averaged rainfall rate $P_t(x,y)$; the map of the temporally averaged runoff coefficient $W_t(x,y)$; the map of the temporal covariance $cov_t(P,W)$ between $P(x,y,t)$ and $W(x,y,t)$; and the map of the temporally averaged rainfall excess rate $R_t(x,y)$.

Table 1
Terms contributing to the storm-averaged catchment rainfall excess [mm/h] of Eq. (4) for the five events of Fig. 2. The terms are shown for two catchments: Kamp at Zwettl and Taffa at Frauenhofen. The important space-time variability terms are shown in bold. The non-relevant terms are shown in grey.

Components of the storm-averaged catchment rainfall excess [mm/h]	August 2002		August 1992		August 1996		April 2006		April 1996	
	Long-rain		Short-rain		Short-rain		Rain-on-snow		Snowmelt	
	Zwettl	Frauen.	Zwettl	Frauen.	Zwettl	Frauen.	Zwettl	Frauen.	Zwettl	Frauen.
$P_{x,y,t}$	4.33	4.43	2.28	1.98	1.15	1.16	0.519	0.686	0.321	0.316
$W_{x,y,t}$ []	0.435	0.190	0.0305	0.00737	0.0367	0.00943	0.443	0.450	0.436	0.311
R1 $P_{x,y,t} \cdot W_{x,y,t}$	1.89	0.840	0.0696	0.0146	0.0422	0.0110	0.230	0.309	0.140	0.0982
R2 $cov_t(P_{x,y}, W_{x,y})$	-0.160	-0.119	0.00624	0.00355	-0.00131	0.00146	-0.0018	0.0057	-0.0002	-0.0002
R3 $cov_{x,y}(P_t, W_t)$	0.0105	0.0105	0.00982	-0.00054	0.00773	-0.00039	0.0002	0.0499	0.0034	0.0131
R4 $[cov_t(P - P_{x,y}, W - W_{x,y})]_{x,y}$	0.0003	-0.0231	0.00025	-0.00006	-0.00273	0.00022	0.0022	0.0023	0.0001	0.0008
R4 - R2-R3/R1 Movement	0.0012	-0.0216	-0.00063	0.00007	-0.00249	0.00027	0.0021	0.0013	0.0001	0.0009
R1 + ... + R4 $R_{x,y,t}$	1.74	0.708	0.0859	0.0175	0.0459	0.0123	0.230	0.367	0.143	0.112

network routing on the time at which the rainfall excess exits a basin. Water that passes a catchment outlet goes through three successive stages in our conceptualisation: (i) the generation of runoff at a point (including waiting for the rain to fall), (ii) hillslope routing and (iii) channel routing. Each of these stages has an associated “holding time”, which is conveniently treated as a random variable (e.g., Rodriguez-Iturbe and Valdes, 1979). Catchment runoff time itself is treated as a random variable (denoted as T_q), which measures the time from the storm beginning until a drop of water exits the catchment. Since the water exiting the catchment has passed in sequence through the three stages mentioned above we can write

$$T_q = T_r + T_h + T_n$$

where T_r , T_h and T_n are the holding times for rainfall excess, hillslope travel and network travel. Using the mass conservation property (see Viglione et al., 2010) we can write the mean of T_q as

$$E(T_q) = E(T_r) + E(T_h) + E(T_n) \tag{5}$$

which represents the mean runoff time of the catchment. The variance of T_q , which represents the dispersion (the inverse of the peakedness) of the hydrograph, is

$$\begin{aligned} \text{Var}(T_q) = & \text{Var}(T_r) + \text{Var}(T_h) + \text{Var}(T_n) + 2\text{Cov}(T_r, T_h) + \\ & + 2\text{Cov}(T_r, T_n) + 2\text{Cov}(T_h, T_n) \end{aligned} \tag{6}$$

The analytical forms of the terms in Eqs. (5) and (6) are shown hereafter (see Viglione et al., 2010, for the derivation of them).

3.2.1. Mean catchment runoff time

3.2.1.1. Mean runoff generation time. The mean runoff generation time is given by:

$$E(T_r) = \underbrace{\frac{T_m}{2}}_{E_{r1}} + \underbrace{\frac{\text{cov}_t(T, R_{x,y})}{R_{x,y,t}}}_{E_{r2}} \tag{7}$$

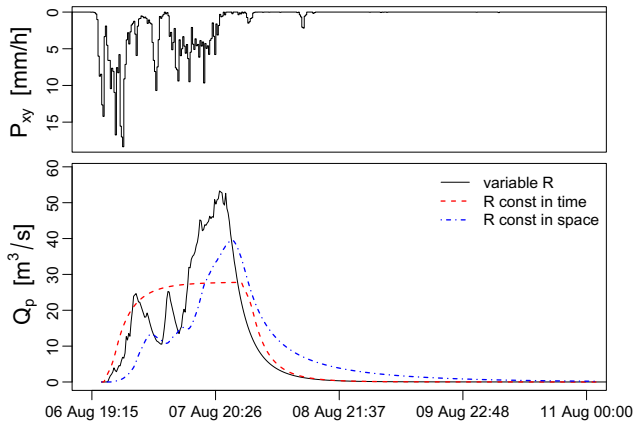


Fig. 5. Runoff time series $Q(t)$ simulated using the assumptions of the analytical framework vs. what have been resulted if rainfall excess were assumed constant in time ($R(x,y,t) = R_t(x,y)$) or in space ($R(x,y,t) = R_{xy}(t)$). The long-rain event of August 2002 in Frauenhofen is shown.

where T_m is the duration of the rainfall event, T is time measured since the start of the rainfall event, R_{xy} is given by Eq. (2) and $R_{x,y,t}$ is given by Eq. (4). The two terms in Eq. (7) are:

- (Er1) half of the duration of the rainfall event [T];
- (Er2) effects of the temporal correlation in rainfall and runoff generation processes [T], which accounts for the additional runoff time that is caused by the temporal variability in rainfall and runoff generation processes, relative to a rain event that generate rainfall excesses at a constant rate throughout the event.

In the top panel of Fig. 5 the temporal evolution of the rainfall event of August 2002 in Frauenhofen (averaged in space) is shown. The bottom panel shows instead the modelled discharge when spatio-temporal variabilities are considered (continuous black line), when the temporal variability are neglected (dashed red¹ line) and when the spatial variabilities are neglected (dashed-dotted blue line). In the case represented in Fig. 5, neglecting the temporal variability in rainfall and runoff generation processes would result in a much smoothed hydrograph with smaller average runoff time. For this event, therefore, the term Er2 is positive (see Table 2) meaning that the average runoff time is higher than would be produced by constant rainfall excess (i.e., by a rectangular storm).

3.2.1.2. Mean hillslope travel time. We assume that the hillslope response can be modelled as a linear reservoir with response time $t_h(x,y)$ constant in time but variable in space (see Viglione et al., 2010). We can express the delay of the hillslope routing as

$$E(T_h) = \underbrace{[t_h]_{x,y}}_{Eh1} + \underbrace{\frac{\text{cov}_{xy}(t_h, R_t)}{R_{x,y,t}}}_{Eh2} \quad (8)$$

The two terms in Eq. (8) are:

- (Eh1) average hillslope travel time [T], i.e., the average time taken for rainfall excess to travel from a location where rainfall excess was generated to the base of the hillslope;
- (Eh2) space variability term related to the hillslope routing [T], which accounts for the additional hillslope-routing time that

is caused by the spatial variability in rainfall excess, relative to a rain event that generate rainfall excess uniformly over the catchment.

3.2.1.3. Mean network travel time. Analogously to Eq. (8), the delay of the channel routing can be derived as

$$E(T_n) = \underbrace{\frac{D_{x,y}}{v}}_{En1} + \underbrace{\frac{\text{cov}_{xy}(D, R_t)}{v \cdot R_{x,y,t}}}_{En2} \quad (9)$$

where $D(x,y)$ [L] is the spatial pattern of flow distances to the catchment outlet and we assume that a unique flow celerity v [LT^{-1}] exists for all travel paths across the catchment. The two terms in Eq. (9) are:

- (En1) average travel time in the channel network [T];
- (En2) space variability term related to the channel routing [T], which accounts for the additional channel-routing time that is caused by the spatial variability in rainfall excess, relative to a rain event that generate rainfall excess uniformly over the catchment.

The mean flow distance $D_{x,y}$ in the first term can be adequately estimated in many cases from the catchment area without detailed network data by using empirical relationships similar to Hack's law (e.g., Robinson et al., 1995) and the order-of-magnitude estimates for channel velocity v are typically 1 m/s. In the bottom panel of Fig. 5 the modelled discharge when the spatial variabilities are neglected is shown by the dashed-dotted blue line. For this event, August 2002 in Frauenhofen, the average catchment runoff time would be slightly higher when neglecting the spatial variabilities, so the sum of terms Eh2 and En2 is negative. Table 2 shows that only Eh2 is considerable for Frauenhofen, meaning that the catchment runoff time is small because runoff is produced mainly on the fast responding hillslopes and not because it is produced close to the outlet, which is confirmed by looking at Fig. 6.

3.2.2. Variance of catchment runoff time

3.2.2.1. Variance of runoff generation time. The variance of the time of rainfall excess is

$$\text{Var}(T_r) = \underbrace{\frac{T_m^2}{12}}_{Vr1} + \underbrace{\frac{\text{cov}_t[T^2, R_{xy}(T)]}{R_{xy,t}} - \frac{\text{cov}_t[T, R_{xy}(T)]}{R_{xy,t}} \left[T_m + \frac{\text{cov}_t[T, R_{xy}(T)]}{R_{xy,t}} \right]}_{Vr2} \quad (10)$$

The two terms in Eq. (10) are:

- (Vr1) variance of the rainfall excess time series if it was steady throughout the event [T^2] (i.e., longer rain events cause greater variance in runoff time, and therefore more dispersed hydrographs, than short-rain events, other things being equal);
- (Vr2) additional variance in the rainfall excess time series that is caused by the temporal variability in rainfall and runoff generation processes, relative to a rain event that generate rainfall excess at a constant rate throughout the event [T^2].

The term Vr2 can be negative, signifying that the patterns of rainfall excess have concentrated the catchment response in time. In the case represented in Fig. 5, neglecting the temporal variability in rainfall and runoff generation processes would result in a much smoothed hydrograph. For this event, therefore, the term Vr2 is negative (see Table 3).

¹ For interpretation of color in Figs. 1, 3, 5, 8 and 9, the reader is referred to the web version of this article.

Table 2
The terms [h] contributing to the mean runoff time of Eq. (5) for the five events of Fig. 2. The terms are shown for two catchments: Kamp at Zwettl and Taffa at Frauenhofen. The important space-time variability terms are shown in bold. The non-relevant terms are shown in grey.

Components of the mean catchment runoff time [h]			August 2002 Long-rain		August 1992 Short-rain		August 1996 Short-rain		April 2006 Rain-on-snow		April 1996 Snowmelt	
			Zwettl	Frauen.	Zwettl	Frauen.	Zwettl	Frauen.	Zwettl	Frauen.	Zwettl	Frauen.
Runoff generation	Er1	$T_m/2$	21.0	14.0	6.75	6.75	16.6	16.6	141	51.5	79.0	79.0
	Er2	Temporal variab. of $R_{x,y}$	0.130	3.24	1.91	2.55	1.12	7.45	-8.13	9.56	-1.62	-3.98
	Er1 + Er2	$E(T_r)$	21.1	17.2	8.66	9.30	17.7	24.1	132	61.1	77.4	75.0
Hillslope routing	Eh1	$[t_{h,x,y}]$	9.87	9.86	29.6	39.4	19.7	39.4	19.7	9.86	19.7	9.86
	Eh2	Spatial variab. of t_h vs. R_t	-0.113	-6.35	-16.3	-33.8	-9.64	-33.5	-0.01	-4.63	-1.57	-6.06
	Eh1 + Eh2	$E(T_h)$	9.76	3.50	13.3	5.61	10.1	5.96	19.7	5.22	18.2	3.80
Channel routing	En1	$D_{x,y}/v$	4.19	2.04	10.5	2.04	10.5	2.04	4.19	2.04	4.19	2.04
	En2	Spatial variab. of D vs. R_t	-0.309	0.065	-3.34	-0.683	-4.99	-0.627	-0.37	0.33	-0.32	0.16
	En1 + En2	$E(T_n)$	3.88	2.10	7.13	1.35	5.48	1.41	3.81	2.36	3.87	2.17
	Er1 + ... + En2	$E(T_q)$	34.8	22.8	29.1	16.3	33.3	31.4	156	68.6	99.4	81.0
		Mean response time	17.5	10.7	21.3	7.99	17.4	11.9	30.3	9.52	21.9	9.84

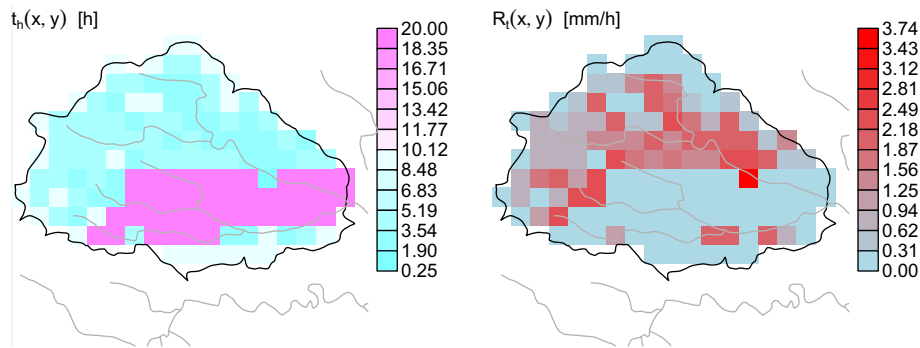


Fig. 6. Spatial distribution of the hillslope runoff time $t_h(x,y)$ compared to the storm-averaged rainfall excess $R_t(x,y)$. The long-rain event of August 2002 in Frauenhofen is shown.

3.2.3. Variance of hillslope travel time

We assume that the hillslope routing can be modelled as a linear reservoir with response time $t_h(x,y)$ constant in time but variable in space, therefore the variance of the delay of the hillslope routing is:

$$\text{Var}(T_h) = \underbrace{[t_{h,x,y}^2]}_{Vh1} + \underbrace{\text{var}_{x,y}(t_h)}_{Vh2} + \underbrace{2 \frac{\text{cov}_{x,y}[t_h^2, R_t]}{R_{x,y,t}} - \frac{\text{cov}_{x,y}[t_h, R_t]}{R_{x,y,t}} \cdot [2[t_h]_{x,y} + \frac{\text{cov}_{x,y}[t_h, R_t]}{R_{x,y,t}}]}_{Vh3} \quad (11)$$

where the three terms are:

- (Vh1) spatial average of the variance of the hillslope routing time $[T^2]$ (variance of the linear reservoir/exponential distribution);
- (Vh2) spatial variance of the hillslope response time $[T^2]$;
- (Vh3) additional variance in hillslope-routing time that is caused by the spatial variability in rainfall excess, relative to a rain event that generate rainfall excess uniformly throughout the basin $[T^2]$.

The term Vh3 can be negative, signifying that the patterns of rainfall excess have concentrated the catchment response in space.

3.2.4. Variance of network travel time

The variance of the delay of the channel routing is, following the same reasoning, as:

$$\text{Var}(T_n) = \underbrace{\frac{\text{var}_{x,y}(D)}{v^2}}_{Vn1} + \underbrace{\frac{\text{cov}_{x,y}[D^2, R_t]}{v^2 R_{x,y,t}} - \frac{\text{cov}_{x,y}[D, R_t]}{v R_{x,y,t}} \cdot [2 \frac{D_{x,y}}{v} + \frac{\text{cov}_{x,y}[D, R_t]}{v R_{x,y,t}}]}_{Vn2} \quad (12)$$

where the two terms are:

- (Vn1) variance of travel time in the channel network $[T^2]$, thus a catchment with a wide range of flow distances to the outlet is predicted to have a large variance in runoff time (see Rinaldo et al., 1991);
- (Vn2) additional variance in channel-routing time that is caused by the spatial variability in rainfall excess, relative to a rain event that generate rainfall excess uniformly throughout the basin $[T^2]$.

This second term can be negative, signifying that the patterns of rainfall excess have concentrated the catchment response in space. In the case represented in Fig. 5, neglecting the spatial variability in rainfall and runoff generation processes would result in a much smoothed hydrograph (with a fat recession curve). Looking at Table 3, one sees that Vh3 is the most relevant spatial variability term meaning that the hydrograph is peaky because runoff is produced mainly on hillslopes with similar response time, which is

Table 3
The terms [h²] contributing to the variance of runoff time of Eq. (6) for the five events of Fig. 2. The terms are shown for two catchments: Kamp at Zwettl and Tafra at Frauenhofen. The important space-time variability terms are shown in bold. The non-relevant terms are shown in grey.

Components of variance of the catchment runoff time [h ²]		August 2002		August 1992		August 1996		April 2006		April 1996	
		Zwettl	Frauen.	Zwettl	Frauen.	Zwettl	Frauen.	Zwettl	Frauen.	Zwettl	Frauen.
Runoff generation	Vr1	147	65.3	15.1	15.1	92.0	92.0	6580	884	2080	2080
	Vr2	-78.7	-22.3	-9.25	-10.1	-33.1	-33.1	-2277	-101	-499	-597
	Vr1 + Vr2	68.2	42.9	5.85	4.97	59.0	59.0	4303	783	1582	1483
Hillslope routing	Vh1	118	147	1058	2345	470	2345	470	147	470	147
	Vh2	20.1	49.4	181	790	80.3	790	80.3	49.4	80.3	49.4
	Vh3	22.1	-175	-667	-2951	-140	-2974	98.7	-153	-22.1	-171
Channel routing	Vh1 + Vh2 + Vh3	160	20.7	571	185	410	162	649	43	528	24.5
	Vn1	3.66	0.92	22.9	0.92	22.9	0.92	3.7	0.9	3.7	0.9
	Vn2	0.28	-0.17	-0.69	-0.38	-1.62	-0.36	-0.1	-0.2	-0.1	-0.2
Covariances	Vn1 + Vn2	3.94	0.75	22.2	0.54	21.3	0.57	3.6	0.7	3.7	0.7
	2 Crh	-2.72	4.49	8.00	1.26	68.2	10.3	24.1	15.1	35.2	3.9
	2 Crn	5.12	0.41	1.02	0.25	17.9	1.90	44.9	2.5	-4.8	9.2
Covariances	2 Chn1	-3.06	-4.35	-23.0	-17.4	-15.3	-17.4	-6.1	-4.3	-6.1	-4.3
	2 Chn2	-1.48	5.01	79.6	23.5	40.9	22.9	-6.2	5.0	1.6	4.2
	2 (Chn1 + Chn2)	-4.55	0.67	56.6	6.16	25.6	5.54	-12.3	0.6	-4.6	-0.1
	Vr1 + ... + 2 Chn2	230	70.0	665	198	656	239	5012	846	2139	1521
	Var(T _q)										

confirmed by looking at Fig. 6. In this case the runoff is produced on fast responding hillslopes but the spatial variability term would have been negative also in the case of runoff produced mainly on slow responding hillslopes. In that case the release would have been delayed in time (would have increased E(T_h)), but concentrated to give a peaky response.

3.2.4.1. Covariances of runoff generation time with hillslope and network travel times. The covariance between rainfall excess time and hillslope-routing time Cov(T_r, T_h) [T²] accounts for the additional variance of the runoff time because of the correlation between time of runoff production and the spatial variability of hillslope response time. This covariance can be written as:

$$\text{Cov}(T_r, T_h) = \underbrace{\frac{\text{cov}_t[T, \text{cov}_{x,y}(t_h, R)]}{R_{x,y,t}}}_{\text{Crh}} - \underbrace{\frac{\text{cov}_t(T, R_{x,y})}{R_{x,y,t}} \frac{\text{cov}_{x,y}(t_h, R_t)}{R_{x,y,t}}}_{\text{Crn}} \quad (13)$$

The difference of the two terms is the covariance of time, runoff generation and hillslope response time due to the movement of runoff generation over the catchment, i.e., storm movement and shift of runoff generation properties.

Analogously, the covariance between rainfall excess time and network routing time Cov(T_r, T_n) [T²], which accounts for the additional variance of the runoff time because of the correlation between time runoff production and the time in the channel network, can be written as:

$$\text{Cov}(T_r, T_n) = \underbrace{\frac{\text{cov}_t[T, \text{cov}_{x,y}(D, R)]}{vR_{x,y,t}}}_{\text{Crn}} - \underbrace{\frac{\text{cov}_t(T, R_{x,y})}{R_{x,y,t}} \frac{\text{cov}_{x,y}(D, R_t)}{vR_{x,y,t}}}_{\text{Crn}} \quad (14)$$

As in Eq. (13), the difference of the two terms is the covariance of runoff generation, distance to the outlet and time due to the movement of runoff generation.

3.2.5. Covariance between hillslope and network travel times

The term Cov(T_h, T_n) [T²] accounts for the additional variance of the runoff time because of the spatial correlation between hillslope response time and the time in the channel network. This covariance can be written as:

$$\text{Cov}(T_h, T_n) = \underbrace{\frac{\text{cov}_{x,y}(t_h, D)}{v}}_{\text{Chn1}} + \underbrace{\frac{\text{cov}_{x,y}(t_h \cdot D, R_t)}{vR_{x,y,t}} - [t_h]_{x,y} \frac{\text{cov}_{x,y}(D, R_t)}{vR_{x,y,t}}}_{\text{Chn2}} - \underbrace{\frac{D_{x,y}}{v} \frac{\text{cov}_{x,y}(t_h, R_t)}{R_{x,y,t}} - \frac{\text{cov}_{x,y}(D, R_t)}{vR_{x,y,t}} \frac{\text{cov}_{x,y}(t_h, R_t)}{R_{x,y,t}}}_{\text{Chn2}} \quad (15)$$

where the two terms are:

- (Chn1) the variance of T_q caused by the spatial covariance between hillslope response time and distance to the outlet [T²];
- (Chn2) the additional variance of T_q caused by joint correlation of t_h(x,y), D(x,y) and the storm-averaged rainfall excess R_t(x,y), relative to a rain event that generate rainfall excess uniformly throughout the basin [T²].

Cov(T_h, T_n) is essentially a spatial term because time does not appear in Eq. (15). Considering the short-rain event of August 1992 in Zwettl represented in Fig. 7, the hillslope response time t_h(x,y) is particularly high close to the outlet only. This determines a negative value for Chn1 (see Table 3 in the results section). However, the runoff is generated on fast responding hillslopes only (close to streams) and is very low on the slow responding hillslopes close to the outlet. Therefore Chn2 is positive.

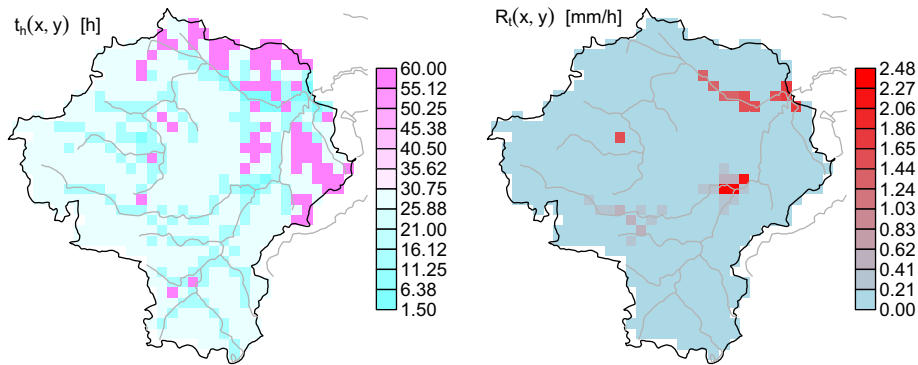


Fig. 7. Spatial distribution of the hillslope response time $t_h(x,y)$ compared to the storm-averaged rainfall excess $R_t(x,y)$. The short-rain event of August 1992 in Zwettl is shown.

4. Results

4.1. August 2002 – long-rain event

In August 2002 a Vb-cyclone (Mudelsee et al., 2004) carried warm moist air from the Adriatic region and caused persistent rainfall over the Kamp region. More than 180 mm of rainfall fell in 42 h on the Zwettl and Neustift catchments with local amounts of more than 300 mm. On Rastenberg the rain was 200 mm, while on Frauenhofen 124 mm fell in 28 h. In Zwettl, this resulted in a peak flow of 460 m³/s which is three times the second largest flood on record (Reszler et al., 2008; Merz and Blöschl, 2008a; Merz and Blöschl, 2008b). The average storm intensity $P_{x,y,t}$ was more than 4 mm/h everywhere. Antecedent rainfall was the cause of the saturation of the catchment: according to the Kamp model parameterisation, the value of the event-catchment runoff coefficient $W_{x,y,t}$ was more than 0.4 for all the catchments except Frauenhofen, where it was 0.19. The average hillslope-routing time has been assumed equal to 10 h in Zwettl and Neustift, 8 h in Rastenberg and 5 h in Frauenhofen. These values are consistent with the average fast-response time of the cells of the calibrated Kamp model. The faster hillslope-routing time in Frauenhofen is due to the connection of hillslopes to the streams because of agricultural use of the land. The stream velocity v has been assumed equal to 1.5 m/s everywhere. This value for the stream velocity has been chosen manually so to match the observed hydrograph with the discharge modelled according to the assumptions of our framework (in a

way, v has been calibrated). In Fig. 8 it is shown, to provide an example, how the hydrograph would look like under the assumptions of Sections 3.1 and 3.2 compared to the observed hydrograph and the one obtained using the distributed Kamp model. Obviously the recession curve is underestimated because in our framework we just model the flood runoff (the fast response) and not the base-flow, which is instead modelled by the Kamp model. It is important to note, again, that our framework is not intended to be a predictive model but a tool that can quantify the relative importance of the processes involved in flood response and the space-time interactions between rainfall and catchment state during flood events.

The terms of Eq. (4), for the storm-averaged catchment rainfall excess, are reported in Table 1. For reasons of space, the values are reported for only two of the four catchments, i.e., Kamp at Zwettl and Taffa at Frauenhofen (a summary of the results for all four catchments is given in the summary Table 4). The term of temporal covariance $\text{cov}_t(P_{x,y}, W_{x,y})$ is significant, corresponding to -9% of $R_{x,y,t}$ in Zwettl and -17% in Frauenhofen. This means that it was raining a lot when the runoff coefficient was low (in the first part of the event). On the contrary, the term of spatial covariance $\text{cov}_{x,y}(P_t, W_t)$ is very low, meaning that there is no particular correlation between the spatial pattern of rainfall and runoff coefficient, i.e., it was not raining particularly low/high where the runoff coefficient is particularly low/high. This means that, for runoff generation, spatially distributed description of precipitation and runoff coefficient is not necessary, therefore a model lumped in space would have been good enough. What is important, especially in Frauenhofen, is the temporal evolution of rainfall and runoff coefficient.

As shown in Table 2, in which the terms of Eq. (5) are listed, the mean runoff time $E(T_q)$ is mainly controlled by storm duration, with significant contribution of hillslope and channel routing delays. The covariance terms $\text{Er}2$, $\text{Eh}2$ and $\text{En}2$ do not play a relevant role in Zwettl, Rastenberg and Neustift. Only in Frauenhofen the temporal variability term $\text{Er}2$ contributes for about $+14\%$ to $E(T_q)$ meaning that a further delay of T_q occurs because the rainfall excess is more important in the second part of the event. In Frauenhofen, also the hillslope variability term $\text{Eh}2$ is considerable (-28%). In Fig. 6 the spatial distribution of the hillslope response time t_h and the storm-averaged rainfall excess $R_t(x,y)$ are compared for Frauenhofen. As can be seen, the runoff was generated mostly where the hillslope response time was small, this determining a faster overall catchment response. Thus, in Frauenhofen, spatially distributed description of runoff generation is important to evaluate the average runoff time $E(T_q)$ (a distributed model is therefore necessary). The channel spatial variability term $\text{En}2$ is low for all catchments meaning that there is no particular correlation between runoff generation and distance to the outlet (which can be

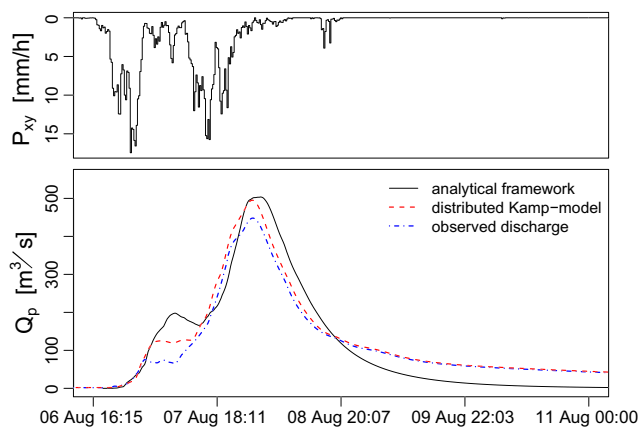


Fig. 8. Runoff time series $Q(t)$: measured, simulated by the Kamp-model, simulated using the assumptions of the analytical framework. The long-rain event of August 2002 in Zwettl is shown.

Table 4
Summary table: important components for the five events of Fig. 2 and for the four catchments in Fig. 1. For the meaning of the components, see Eqs. (4) and (15) and Tables 1–3.

	August 2002 Long-rain	August 1992 Short-rain	August 1996 Short-rain	Short-rain	April 2006 Rain-on-snow	April 1996 Snowmelt
Zwettl	$R_{xy,t}$ $E(T_q)$ $Var(T_q)$	R1, R2, R3 Er1, Er2, Eh1, Eh2, En1, En2 Vr1, Vh1, Vh2, Vh3, Vn1, 2 Chn1, 2 Chn2	R1, R2, R3, R4 Er1, Er2, Eh1, Eh2, En1, En2 Vr1, Vr2, Vh1, Vh2, Vh3, Vn1, 2 Crh, 2 Chn2	R1, R2, R3, R4 Er1, Er2, Eh1, Eh2, En1, En2 Vr1, Vr2, Vh1, Vh2, Vh3, Vn1, 2 Crh, 2 Chn2	R1 Er1, Er2, Eh1, Eh2, En1, En2 Vr1, Vr2, Vh1, Vh2, Vh3	R1 Er1, Er2, Eh1, Eh2, En1, En2 Vr1, Vr2, Vh1, Vh2, Vh3
Rastenberg	$R_{xy,t}$ $E(T_q)$ $Var(T_q)$	R1, R2 Er1, Eh1, En1 Vr1, Vr2, Vh1, Vh2, Vh3	R1, R2, R3 Er1, Er2, Eh1, Eh2, En1 Vr1, Vr2, Vh1, Vh2, Vh3, Vn1, 2 Chn2	R1, R3, R4 Er1, Er2, Eh1, Eh2, En1, En2 Vr1, Vh1, Vh2, Vh3, Vn1, 2 Crh, 2 Chn2	R1 Er1, Er2, Eh1 Vr1, Vr2, Vh1	R1, R3 Er1, Eh1 Vr1, Vr2, Vh1, Vh2, Vh3
Neustift	$R_{xy,t}$ $E(T_q)$ $Var(T_q)$	R1, R2 Er1, Er2, Eh1, En1 Vr1, Vr2, Vh1, Vh2, Vh3	R1, R2, R3 Er1, Er2, Eh1, Eh2, En1, En2 Vr1, Vh1, Vh2, Vh3	R1, R2 Er1, Er2, Eh1, Eh2, En1 Vr1, Vh1, Vh2, Vh3, Vn1	R1, R3 Er1, Er2, Eh1 Vr1, Vr2, Vh1	R1 Er1, Er2, Eh1 Vr1, Vr2, Vh1
Frauenhofen	$R_{xy,t}$ $E(T_q)$ $Var(T_q)$	R1, R2 Er1, Er2, Eh1, Eh2, En1 Vr1, Vr2, Vh1, Vh2, Vh3	R1, R2, R3 Er1, Er2, Eh1, Eh2, En1, En2 Vr1, Vr2, Vh1, Vh2, Vh3, 2 Chn1, 2 Chn2	R1, R2, R3, R4 Er1, Er2, Eh1, Eh2 Vr1, Vr2, Vh1, Vh2, Vh3, 2 Crh, 2 Chn1, 2 Chn2	R1, R3 Er1, Er2, Eh1, Eh2, En1 Vr1, Vr2, Vh1, Vh2, Vh3	R1, R3 Er1, Er2, Eh1, Eh2 Vr1, Vr2, Vh1, Vh2, Vh3

seen in Fig. 6 as well). The last row in Table 2 is the mean catchment response time, i.e., the delay between the centroids of rainfall and runoff, which is calculated subtracting the mean rainfall time to the mean catchment runoff time $E(T_q)$.

The terms of Eq. (6), which give the variance of the runoff time $Var(T_q)$, are shown in Table 3. $Var(T_q)$ is controlled by the variance of the runoff production time $Var(T_r)$ and the variance of the hillslope routing time $Var(T_h)$. In particular, the temporal variability term Vr2 is very negative (e.g. correspond to -59% of $Var(T_q)$ for Neustift) meaning that the peakedness of the hydrograph is much higher than what would be produced by a constant runoff generation in time (if $R(x,y,t) = R_t(x,y)$, see Fig. 5 for Frauenhofen). Essentially the rainfall time pattern concentrates in time the runoff production. The hillslope term $Var(T_h)$ is very high in Zwettl and Rastenberg and particularly low in Frauenhofen. For all these catchment Vh2 is significantly high, because of the variability of t_h in space. The spatial variability term Vh3 is positive in Zwettl and Rastenberg, i.e., the spatial variability of the hillslope response time, coupled with the spatial variability of runoff production, smooths down the hydrograph. On the contrary, Vh3 is very negative in Frauenhofen, meaning that there the peakedness of the hydrograph is much higher than what would be produced by a constant runoff generation in space (if $R(x,y,t) = R_{x,y}(t)$, see Fig. 5). In Frauenhofen, in fact, almost all runoff is produced on fast responding hillslopes, thus concentrating the overall response in time (see Fig. 6). The flow distance term Vn1 and channel spatial variability term Vn2 are irrelevant. Among the other terms, $Cov(T_r, T_h)$ is significant in Frauenhofen only (+6% of $Var(T_q)$). This means that the movement of the storm plays a role there, in relation to the spatial distribution of t_h .

4.2. August 1992 – short-rain event

The second event analysed here is the convective thunderstorm of August 1992. The flood event was small: 8m³/s were measured in Zwettl. On Zwettl and Neustift, 30–36 mm of rainfall fell in 13.5 h with local amounts of more than 50 mm. On Rastenberg and Frauenhofen the total rain was about 25 mm with local amounts of about 35 mm over 13.5 h. The average storm intensity $P_{x,y,t}$ is close to 2 mm/h or more (e.g., Neustift is the catchment with the highest average storm intensity, see Table 1). The catchments condition at the beginning of the event were dry and, therefore, the value of the event-catchment runoff coefficient $W_{x,y,t}$ is low for all the catchments, in particular for Frauenhofen. The average hillslope-routing time has been assumed equal to 30 h in Zwettl and Neustift and 20 h in Rastenberg and Frauenhofen. In this short-rain event, the hillslope routing time in Frauenhofen is not fast because rain was falling mainly in the flat area and was captured by the groundwater system. The stream velocity v has been assumed equal to 0.6 m/s in Zwettl, Neustift and Rastenberg, and to 1.5 m/s in Frauenhofen. In Frauenhofen, in fact, the network is mainly made of regulated channels in which, when the amount of water is small, the velocities are much higher than in natural streams.

For Zwettl and Neustift, the term of spatial covariance $cov_{xy}(P_t, W_t)$ is relevant, corresponding to +11% and +12% of $R_{x,y,t}$ respectively (see Table 1 for Zwettl). This means that it was raining more intensely where the runoff coefficient was relatively high. The term of temporal covariance $cov_t(P_{x,y}, W_{x,y})$ is considerable in Frauenhofen, corresponding to +20% of $R_{x,y,t}$. This means that it was raining more intensely when the runoff coefficient was relatively high (in the second part of the event). The movement of the storm, which was quite stationary, had no effect on runoff production.

The mean runoff time $E(T_q)$ (see Table 2) is controlled, in order of importance, by hillslope routing, storm duration and channel routing except in Frauenhofen, where storm duration is the most

important component. The temporal variability term $Er2$ contributes everywhere for more than +6% to $E(T_q)$ ($\sim +16\%$ in Frauenhofen) meaning that a further delay of T_q occurs because the rainfall excess is more important in the second part of the event (after $T_m/2$). The hillslope spatial variability term $Eh2$ is very negative everywhere (in particular in Frauenhofen), meaning that the runoff was generated mostly where the hillslope response time is small, thus determining a faster overall catchment response (see Fig. 7). The channel spatial variability term $En2$ is lower but corresponds to -11% of $E(T_q)$ for Zwettl, meaning that the rainfall excess was high close to the catchment outlet (i.e., the centroid of the rainfall excess is closer to the catchment outlet than the centroid of the catchment, following the drainage directions), as can be seen in Fig. 7.

The variance of the runoff time $Var(T_q)$ (see Table 3) is controlled by hillslope routing. Deeper flow paths coupled with slower dry hillslopes caused slower subsurface flow. The temporal variability term $vr2$ plays hardly any role for this short-rain event. The hillslope spatial variability term $Vh3$ is very important, meaning that the peakedness of the hydrograph would change a lot (would be less peaky) if one instead assumed a constant runoff generation in space (i.e., if $R(x,y,t) = R_{x,y}(t)$). The runoff is produced mainly on the fast responding hillslopes (see Fig. 7), so that they release the water at the same time concentrating the response in time. In Zwettl and Rastenberg, also $Cov(T_h, T_n)$ is significant. In Zwettl, in particular, the term $Chn1$ is negative because the hillslope response time $t_h(x,y)$ is particularly high close to the outlet. However, the runoff is generated on fast responding hillslopes only (close to streams) and is very low on the slow responding hillslopes close to the outlet. Therefore $Chn2$ is positive and greater than $Chn1$, so that $Cov(T_h, T_n)$ is significantly positive. $Cov(T_h, T_n)$ accounts for the fact that the fast responding hillslopes over which runoff is generated are located at different distances from the outlet (they are not concentrated in space). This results in a smoother response. The term $Chn2$ complete the information provided by $Vh3$ (very negative here), which does not account for the position in the catchment, and $Vn2$ (not relevant here), which does not account for the hillslope response time.

4.3. August 1996 – short-rain event

The event of August 1996 was a short-rain double event (see Fig. 2, third row). The resulted flood was rather small: 12 m³/s were measured in Zwettl. On all four catchments 35–45 mm of rainfall fell in 33 h (two parts of about 10 h each, separated by 10 h of no rain) with local amounts of 70 mm in Zwettl and less than 50 in Neustift. The average storm intensity $P_{x,y,t}$ is slightly over 1 mm/h everywhere. The catchments condition at the beginning of the event were dry and, therefore, the value of the event-catchment runoff coefficient $W_{x,y,t}$ was low for all the catchments. The average hillslope-routing time has been assumed equal to 20 h for every catchment. The stream velocity v has been assumed equal to 0.6 m/s in Zwettl, Neustift and Rastenberg, and to 1.5 m/s in Frauenhofen (because of the regulated channels).

The components of the storm-averaged catchment rainfall excess are shown in Table 1. For Zwettl, the term of spatial covariance $cov_{x,y}(P_t, W_t)$ is relevant, corresponding to +17% of $R_{x,y,t}$. This means that it was raining more intensely where the runoff coefficient was relatively high. This can be seen in Fig. 4. The term of temporal covariance $cov_t(P_{x,y}, W_{x,y})$ is relevant in Frauenhofen, corresponding to +12% of $R_{x,y,t}$. This means that it was raining a lot when the runoff coefficient was relatively high (in the second part of the double event). In Zwettl, the term $[cov_t(P - P_{x,y}, W - W_{x,y})]_{x,y}$ is not negligible (-6% of $R_{x,y,t}$). The term $R2$, $cov_t(P_{x,y}, W_{x,y})$, is the temporal covariance between the time series of catchment-averaged rainfall rates $P_{x,y}(t)$ and the time series of catchment-averaged runoff coef-

ficient $W_{x,y}(t)$ represented in Fig. 3 (top panel). It is a measure of the temporal correlation of rainfall and runoff coefficient, which, unlike the term $cov_t(P, W)$ in Eq. (3), ignores the spatial patterns of them. Analogously, the term $R3$, $cov_{x,y}(P_t, W_t)$, is the spatial covariance between the map of the temporally averaged rainfall rates $P_t(x,y)$ and the map of the temporally averaged runoff coefficient $W_t(x,y)$ of Fig. 4. This measures the spatial correlation of rainfall and runoff coefficient but, unlike the term $cov_{x,y}(P, W)$ in Eq. (2), ignores the temporal evolution of the patterns. The spatio-temporal variabilities not accounted for by terms $R2$ and $R3$ are embedded in the term $R4$, i.e., $[cov_t(P - P_{x,y}, W - W_{x,y})]_{x,y}$. As shown in Table 1, $R4$ essentially accounts for the movement of the storm because its absolute value is much higher than $|R2 \cdot R3 / R1|$. The negative value in Zwettl means that rainfall was moving from the wet part of the catchment to the dry part of it, so that when the runoff coefficient increased in the wet part, the storm had already moved away.

The mean runoff time $E(T_q)$ is controlled by all three processes, i.e., storm duration, hillslope routing and channel routing. Hillslope and channel routing are not that important for Frauenhofen (see Table 2) where they accounts for 19% and 4% of the mean runoff time $E(T_q)$ respectively. The temporal variability term $Er2$ is important everywhere (+13% and +24% of $E(T_q)$ in Rastenberg and Frauenhofen respectively) except in Zwettl (+3% of $E(T_q)$). In Zwettl, in fact, the double rainfall event is symmetric, as can be seen in Fig. 3, i.e., not concentrated only before or after $T_m/2$. The hillslope spatial variability term $Eh2$ is negative everywhere (in particular in Frauenhofen) meaning that runoff was generated mostly where the hillslope response time is small, this determining a faster overall catchment response. The channel routing spatial variability term $En2$ is important in Zwettl (-15% of $E(T_q)$) meaning that the runoff was generated close to the outlet of the catchment.

The variance of the runoff time $Var(T_q)$ (see Table 3) is mainly controlled by hillslope routing ($Var(T_h)$ corresponds to more than 60% of $Var(T_q)$ everywhere) and partially by storm duration. The temporal variability term $vr2$ plays a role in Frauenhofen only, where it corresponds to -14% of $Var(T_q)$. It is however interesting to see that the temporal variability term is positive for Zwettl, which arises from the fact that the event was a symmetric double storm event (in Frauenhofen this is not the case because the produced runoff is concentrated almost only in the second part of the event). The hillslope spatial variability term $Vh3$ is very important everywhere meaning that the peakedness of the hydrograph would change a lot (would be less peaky) if one considers a constant runoff generation in space (i.e., if $R(x,y,t) = R_{x,y}(t)$). In Zwettl the two terms accounting for the movement of the runoff generation are important. In particular, $2Cov(T_r, T_h)$ corresponds to +10% of $Var(T_q)$. This is because, in average, runoff was generated early in the event on fast responding hillslopes and later in the event on slow responding hillslopes.

4.4. April 2006 – rain-on-snow event

The event of April 2006 was a rain-on-snow event. Rain was falling on an existing snow cover contributing to enhance snowmelt. The resulting flood was considerable, the peak at Zwettl being 112 m³/s. In the Zwettl, Rastenberg and Neustift catchments, rainfall and snowmelt sum up to about 145 mm in more than 11 days with local amounts between 190 mm in Neustift and 240 mm in Zwettl. In Frauenhofen the considered event is shorter, about 4 days, and rainfall and snowmelt sum up to about 70 mm with local amounts of 130 mm. The average combined rainfall + snowmelt intensity $P_{x,y,t}$ is low everywhere, close to 0.5 mm/h in Zwettl, Rastenberg and Neustift and a little higher in Frauenhofen (see Table 1). Antecedent snowmelt saturated large parts of the catchment facilitating overland flow once rain started.

Thus the value of the event-catchment runoff coefficient $W_{x,y,t}$ was particularly elevated for all the catchments (in Rastenberg is greater than 0.5). The average hillslope-routing time has been assumed equal to 20 h for Zwettl, Rastenberg and Neustift, and equal to 5 h for Frauenhofen. This difference is due to the fact that, in Frauenhofen, the hillslopes are well connected to the streams because of agricultural use of the land. The stream velocity v has been assumed equal to 1.5 m/s everywhere.

The components of the storm-averaged catchment rainfall excess are shown in Table 1. The term of spatial covariance $cov_{xy}(P_t, W_t)$ is significant in Frauenhofen only (+14% of $R_{x,y,t}$), while the term of temporal covariance $cov_t(P_{x,y}, W_{x,y})$ is always unimportant. This is because W is always constant and high in time and P in space (because of the uniform snow cover). The spatially averaged terms of Eq. (2) for Frauenhofen are shown in Fig. 9: one sees that $W_{x,y}$ does not change much in time, which results in unimportant $cov_t(P_{x,y}, W_{x,y})$; the spatial covariance, instead, determines an increase of runoff production, specially in the central part of the event when it does not rain, i.e., snowmelt in the central part of the event occurred more on wetter parts of the catchment.

The mean runoff time $E(T_q)$ (see Table 2) is mainly controlled by the rainfall–snowmelt duration. The temporal variability term $Er2$ is significant, e.g., –9% of $E(T_q)$ for Rastenberg (not shown in the table) and +14% for Frauenhofen. In Rastenberg the runoff generation is more important in the first part of the event, while in Frauenhofen in the second part. This is because of rainfall, which is more concentrated in the first part of the event on Rastenberg and in the second part on Frauenhofen. The hillslope routing term is around +8 ÷ 15% of $E(T_q)$. In Frauenhofen, the mean hillslope travel time is lower than what would result from a spatially uniform runoff production. The term $Eh2$ is negative, meaning that runoff was

generated more on fast responding hillslopes. In all other catchments $Eh2$ is negligible because the runoff generation is uniformly distributed over the catchment. The channel-routing time is everywhere negligible.

The variance of the runoff time $Var(T_q)$ (see Table 3) is controlled by storm duration and temporal variability term with some contribution of the hillslope routing (specially for Rastenberg and Zwettl). The temporal variability term $Vr2$ is negative (e.g., it corresponds to –45% for Zwettl and Rastenberg) meaning that the peakedness of the hydrograph is higher than what would be produced by a constant runoff generation in time (i.e., if $R(x,y,t) = R_t(-x,y)$). The temporal variability of runoff generation is given by the rainfall temporal variability, by the sinusoidal day/night evolution of snowmelt and by the decrease of snowmelt because of the retreat of snow cover (Fig. 9). The temporal variability term $Vr2$ is not so important in Frauenhofen (–12%), where the event is shorter. Here the variance of the hillslope-routing time would be significant if runoff was generated uniformly over the catchment ($Vh1 + Vh2$), but the spatial variability term $Vh3$ compensate for it. All other terms are irrelevant except the moving terms $2 Crh$ and $2 Crr$ in Rastenberg (not shown in the table), which together account for 3% of $Var(T_q)$. These terms reflect not only the movement of rainfall over the catchment but also snowmelt moving from low elevations to high elevations. In particular, low elevations have slower responding hillslopes than high elevations, resulting in the non-negligible term $2 Crh$.

4.5. April 1996 – snowmelt event

The event of April 1996 was a snowmelt event. Rainfall also occurred but was of minor importance. The snowmelt was modelled according to the degree-day concept through the Kamp model. The resulted flood was moderate, the peak at Zwettl being 35 m³/s. In the catchments, the total snowmelt was between 44 and 54 mm over 6 and half days, with local amounts between 55 mm (Neustift) and 80 mm (Frauenhofen). The average snowmelt intensity $P_{x,y,t}$ is low everywhere, less than 0.4 mm/h. Antecedent snowmelt saturated large parts of the catchment facilitating overland flow once rain started. Thus the value of the event-catchment runoff coefficient $W_{x,y,t}$ is elevated for all the catchments. The average hillslope routing time has been assumed equal to 20 h for Zwettl, Rastenberg and Neustift, and equal to 5 h for Frauenhofen. The stream velocity v has been assumed equal to 1.5 m/s everywhere.

The components of the storm-averaged catchment rainfall excess are shown in Table 1. The term of spatial covariance $cov_{xy}(P_t, W_t)$ is relevant in Frauenhofen only (+12% of $R_{x,y,t}$), while the term of temporal covariance $cov_t(P_{x,y}, W_{x,y})$ is always unimportant. This is because W is always constant and high in time and P in space (because of the uniform snow cover).

The mean runoff time $E(T_q)$ (see Table 2) is mainly controlled by the snowmelt duration. In Frauenhofen the temporal and spatial variability terms $Er2$ and $Eh2$ are significant, corresponding to –5% of $E(T_q)$ the first and –7% the second. The hillslope routing term is close to +20% everywhere except in Frauenhofen because of the negative value of the spatial variability term $Eh2$. The channel routing terms are everywhere very low. Only in Zwettl $E(T_n)$ correspond to 4% of $E(T_q)$.

The variance of the runoff time $Var(T_q)$ (see Table 3) is controlled by storm duration with some contribution of the hillslope routing (excluding Frauenhofen). The temporal variability term $Vr2$ is below 0 meaning that the peakedness of the hydrograph is much higher than what would be produced by a constant runoff generation in time (i.e., if $R(x,y,t) = R_t(x,y)$). The temporal variability of runoff generation is given by the sinusoidal day/night evolution of snowmelt and by the decrease of snowmelt because of the retreat of snow cover. The spatial variability term $Vh3$ in

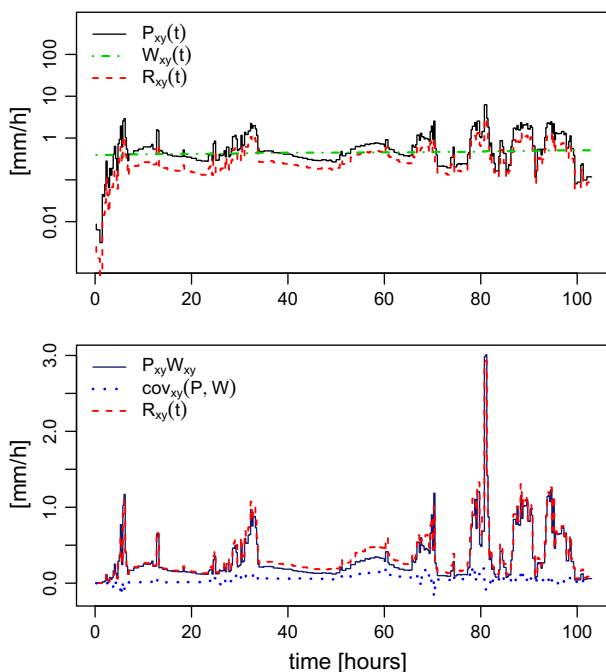


Fig. 9. Instantaneous catchment rainfall excess $R_{xy}(t)$ and components of Eq. (2). The rain-on-snow event of April 2006 in Frauenhofen is shown. The top panel shows, in log-scale: the time series of the catchment-averaged rainfall rate $P_{xy}(t)$; the time series of the catchment-averaged runoff coefficient $W_{xy}(t)$; and the time series of the catchment-averaged rainfall excess rate $R_{xy}(t)$. The bottom panel shows: the time series of the product $P_{xy}(t) \cdot W_{xy}(t)$; the time series of the spatial covariance $cov_{xy}(P, W)$ between $P(x,y,t)$ and $W(x,y,t)$; and the time series of the catchment-averaged rainfall excess rate $R_{xy}(t)$.

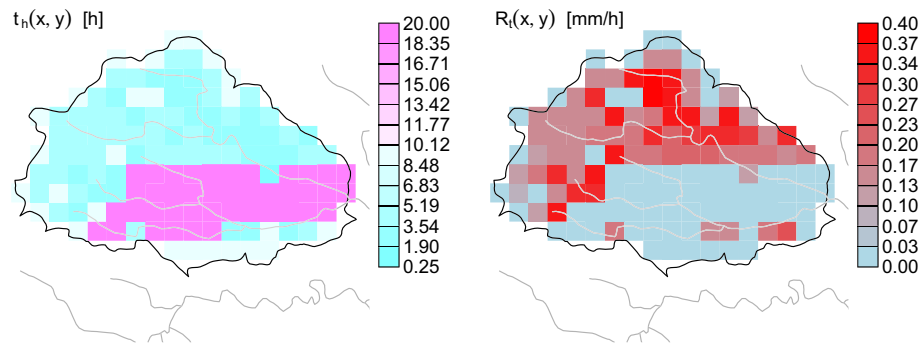


Fig. 10. Spatial distribution of the hillslope response time $t_h(x,y)$ compared to the storm-averaged rainfall excess $R_i(x,y)$. The snowmelt event of April 1996 in Frauenhofen is shown.

Frauenhofen is significant because runoff is generated more on fast responding hillslopes (Fig. 10). All other terms are irrelevant. Only the term $2 Cr_h$ in Zwettl gives a minimal contribution, corresponding to 2% of $\text{Var}(T_q)$. The term reflects snowmelt moving from low elevations to high elevations (in average, low elevations have slower responding hillslopes).

5. Discussion of event types and a dimensionless response number

In the previous sections we showed how an analytical framework (see Viglione et al., 2010, for more details) can be used for exploring the dependence of the catchment flood response characteristics on the spatial and temporal variability of the rainfall patterns, runoff generation and runoff routing across hillslopes and channel network. The catchment response characteristics analysed are: the average rainfall excess rate (Eq. (4)), the mean catchment runoff time (Eq. (5)), and the variance of runoff time (Eq. (6)). In this study, the components of the equations have been calculated for five different types of events in four catchments in the Kamp area in northern Austria. Table 4 lists the components of the equations that are important for the different events and the four catchments.

Regarding runoff production, the long-rain event of August 2002 was characterised by the maximum $R_{x,y,t}$, given the heavy rainfall and the high runoff coefficient over the catchments. The rain-on-snow event of April 2006 gave a higher $R_{x,y,t}$ compared to the snowmelt event of April 1996 because of the highest volume of water involved (precipitation + snowmelt) and also because the runoff coefficients are slightly higher. The two short-rain events, on the contrary, have low precipitation volumes and low runoff coefficients, which results in low runoff production. For these two events, August 1992 and August 1996, both the spatial and temporal variability terms (i.e., R_2 , R_3 and R_4) can be important, which would be expected because of the moderate spatial extent of the storms and their concentration in time. For the event of August 1996 in Zwettl, the movement of the storm contributed non-negligibly to determine the runoff production (which implies that R_4 is important). For the long-rain event of August 2002 the spatial variability term R_3 is irrelevant, which makes sense because the frontal event was spatially uniform and stationary on the area. For the snowmelt and rain-on-snow events the temporal variability term R_2 is negligible, because of the quasi-constant temporal evolution of runoff coefficient, but the spatial variability term R_3 can be important, because of the distribution of snow with altitude.

Regarding the runoff time, the long-rain event of August 2002 is characterised by quite fast and concentrated response. The re-

sponse is slower and much more smoothed for the two short-rain events of August 1992 and August 1996 because of the slower response of hillslopes (giving high values of E_{h1} and V_{h1}). Because of the small amount of water, the connectivity of flow on the surface of the hillslopes was not established determining a slower and dispersed response. In the case of the rain-on-snow and snowmelt events, the delay and smoothness of the produced runoff is due to the long duration and smoothness of rain + snowmelt (giving high values of E_{r1} and V_{r1}). If one considers the mean response times of the catchments, i.e., the delay between the centroid of rainfall (+snowmelt) and produced discharge, they are not so different between event types, ranging between 17.4 h (August 1996) and 30.3 h (April 2006) in Zwettl and between 8 h (August 1992) and 12 h (August 1996) in Frauenhofen. In the short-rain event of August 2002, both temporal and spatial variability terms (the correlation between spatial distribution of runoff generation and hillslope response time) are important for the peakedness of the hydrograph (so V_{r2} , V_{h2} and V_{h3}). Channel routing is not very important for this event, neither for the delay, nor for the spread of the hydrograph, because the associated timescales are small compared to the corresponding runoff production and hillslope timescales. For the short-rain events, the spatial variability of runoff generation is always important (increasing the importance of E_{h2} , E_{n2} , V_{h2} , V_{h3} , $2 Cr_h$, $2 Cr_n$ and $2 Ch_n$, depending on the catchment/event), which is expected because of the local nature of thunderstorms. In all of the catchment, this is related to the spatial distribution of hillslope travel times. In Zwettl, which is the biggest catchment, channel routing also plays a role in these two events. For the event of August 1996 in Zwettl, the movement of the storm contributed non-negligibly in reducing the peakedness of the hydrograph, mainly because, on average, runoff is produced earlier on the fast responding hillslopes, and later on the slowly responding ones (i.e., $2 Cr_h$ is important). In the rain-on-snow and snowmelt events, the temporal variability term V_{r2} is very important in increasing the peakedness of the hydrograph. The value -2277 of the temporal variability term at Zwettl for the event of April 2006 looks like a huge number but is only one third of 6580, i.e., V_{r1} . Event duration (and hence time components) dominates the spread of the hydrograph. The temporal variability terms in Table 3 are negative because runoff production decreases with time as snow melt decreases (the snow cover retreats). It is not the diurnal oscillation of snowmelt that matters, but the time trend within the entire event.

As discussed, the analytical framework gives the magnitudes of the process components in determining some key characteristic of the flood hydrograph. To provide a visual example of the information which two of these characteristics have, i.e., the storm-averaged catchment rainfall excess $R_{x,y,t}$ and the variance of the runoff time $\text{Var}(T_q)$, in Fig. 11 we compare the flood peaks of the

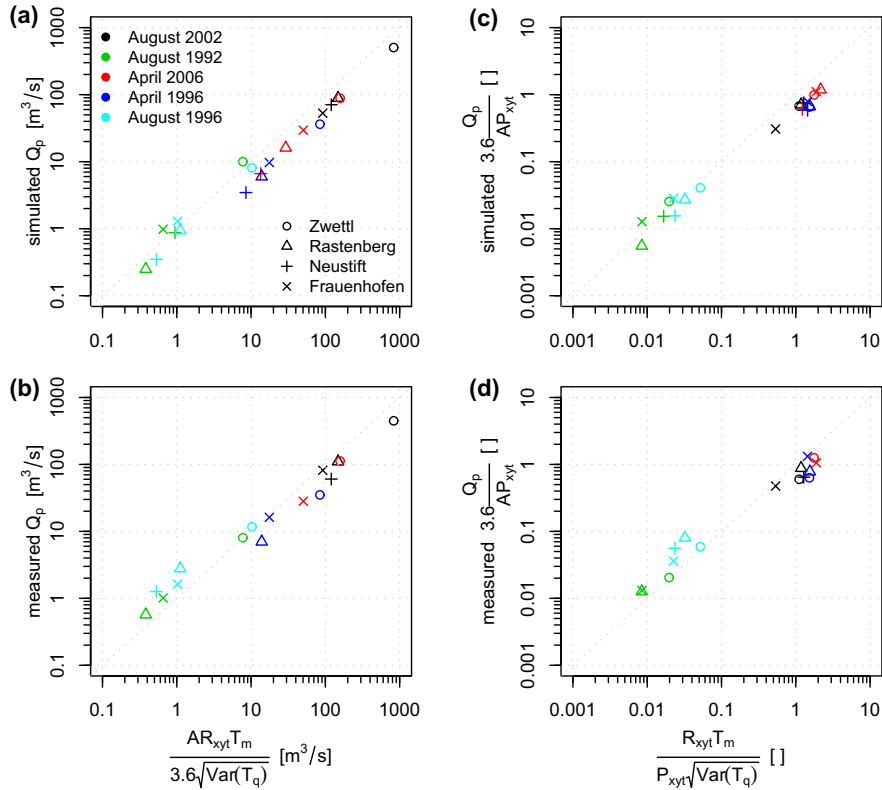


Fig. 11. Response number and dimensionless response number vs. peak discharges in the four catchments for the five events: (a) response number vs. the peak discharge simulated by a distributed model, which follows the assumptions of the analytical framework; (b) response number vs. the observed peak discharge; (c) dimensionless response number vs. the non-dimensional peak discharge simulated by the distributed model; (d) dimensionless response number vs. the non-dimensional observed peak discharge.

five events in the four catchments with a combination of them. A measure of the flood peak can be given by the *response number* [m³/s], which we define as

$$\frac{A \cdot R_{x,y,t} \cdot T_m}{3.6 \cdot \sqrt{\text{Var}(T_q)}} \quad (16)$$

where A [km²] is the catchment area, $R_{x,y,t}$ [mm/h] is the storm-averaged catchment rainfall excess of Eq. (4), T_m [h] is the duration of the storm, $\text{Var}(T_q)$ is the variance of the catchment runoff time of Eq. (6) and 3.6 is for unit conversion. The response number dimensionally corresponds to a discharge and is expected to be related to the flood peak because it accounts for volume and dispersion of the hydrograph. Specifically, $A \cdot R_{x,y,t} \cdot T_m$ is the volume of runoff, and $\sqrt{\text{Var}(T_q)}$ is the characteristic time over which that runoff is distributed, so the ratio of the two may correspond with the peak discharge. Fig. 11a compares the value of the response number with the flood peaks Q_p simulated by a distributed model, which has the same assumptions as the analytical framework. We expect the points of the graph not to follow a 1:1 relationship because the simulated Q_p result from volume, dispersion and other shape characteristics (such as bimodality) of the hydrograph while the response number only accounts for the first two characteristics. Fig. 11, however, shows that the points in Panel (a) lie close to the 1:1 line, which means that the response number captures the magnitude of Q_p very well. Fig. 11b is analogous to Panel (a) where the measured flood peaks Q_p are shown. Since the variables of the framework have been derived from a calibrated model, we expect Panel (b) to be similar to Panel (a), which is the case.

More interesting are Panels (c) and (d). One could argue that the near 1:1 correspondence of the points in Panels (a) and (b) might

be a consequence of catchment areas and rainfall volumes only, in which case the analytical framework provides little new information. In Fig. 11c and d, we therefore compare the non-dimensional peak $3.6 \cdot Q_p / (A \cdot P_{x,y,t})$ [], with the *dimensionless response number* []

$$\frac{R_{x,y,t} \cdot T_m}{P_{x,y,t} \cdot \sqrt{\text{Var}(T_q)}} \quad (17)$$

where $P_{x,y,t}$ is the time- and catchment-averaged precipitation rate [mm/h]. The dimensionless response number originates from the idea of dimensional analysis (see Dooge, 1986; Wagener et al., 2007). It does not depend on the magnitude of the rainfall event and on the catchment size, but on the runoff generation and routing only. It is event runoff coefficient ($R_{x,y,t} \cdot T_m / P_{x,y,t}$) times peakedness ($1/\sqrt{\text{Var}(T_q)}$) and corresponds to the free parameter (often indicated by C) of the rational formula (see e.g., Chow et al., 1988, page 497). The dimensionless response number is also related to the peak discharge response variable of Wood and Hebson (1986) and Robinson and Sivapalan (1997), which was defined for a steady rainfall rate (see also Woods, 1997).

The points in Panels (c) and (d) are also close to the 1:1 line, meaning that the framework captures the dominant features of runoff generation and routing through the catchment. This is a somewhat surprising result because of two reasons. First we would have expected considerable scatter of the relationship in Panels (c) and (d) as the framework used here is only a second moment approximation, while it neglects the higher order moments of the hydrographs. Bimodal and multimodal shapes are non explicitly represented in the framework. Apparently, the approximation works well for the diverse event types (and hydrograph shapes)

examined here. Second there is not only a tight relationship; there is, in fact, a very good 1:1 correspondence. This means that the dimensionless response number also captures the absolute magnitudes of the peaks well. The excellent representation of the peaks for a range of events is a tremendously useful result because the framework allows to capture the components that contribute to the peak of a flood in a natural way, through first and second order moments of rainfall, runoff coefficient, hillslope and channel routing in space and time. Importantly, as shown here, it can be applied to a range of event types, which gives additional relevance to the framework.

The dimensionless response number proposed here is one example of numbers which could be used for dimensional analysis in catchment hydrology, similar to the way the Froude and Reynolds numbers have been used in hydraulics. Potentially, the components obtained using the framework could be combined into other dimensionless numbers. They could be used to establish relationships that are valid over a wide range of scales in the same fashion as the Moody diagram (e.g., Chow et al., 1988). One example in catchment hydrology is provided by Zoccatelli et al. (2010) who use dimensionless numbers from our framework to quantify the effects of spatial and temporal rainfall aggregation on flood response modelling.

The framework discussed in this paper can be used for any type of simulated data, regardless of the actual model employed for generating them. This is a fundamental aspect, since it enables evaluating the role of different process conceptualisations and model structures in the simulated response, and the accuracy with which rainfall events need to be observed for a given type of hydrological model. The framework could be also applied directly to observed data, provided spatial patterns of runoff coefficients are available. At the sub-catchment scale, this could be done in intensively monitored catchments, such as in the MARVEX experiment in New Zealand (Woods et al., 2001). At larger scales, soil moisture from satellite data could be used as a surrogate for the runoff coefficient (Wagner et al., 2007; Wagner et al., 2008).

6. Conclusions

In this paper various flood event types are characterised in terms of the magnitude of the components that contribute to particular hydrograph characteristics (volume, mean time and dispersion in time) and to the peak, through a (dimensionless) response number. The results indicate that the components obtained by the framework clearly reflect the individual processes which characterise the event types. For the short-rain events, temporal, spatial and movement components can all be important in runoff generation and routing, which would be expected because of their local nature in time and, particularly, in space. For the long-rain event, the temporal components tend to be more important for runoff generation, because of the more uniform spatial coverage of rainfall, while for routing the spatial distribution of the produced runoff, which is not uniform, is also important. For the rain-on-snow and snowmelt events, the spatio-temporal variability terms typically do not play much role in runoff generation and the spread of the hydrograph is mainly due to the duration of the event. In addition, the proposed dimensionless response number, which is event runoff coefficient times hydrograph peakedness, captures the absolute magnitudes of the observed flood peaks.

We believe that the main strength of the framework lies in a better understanding of the contributions of the various process components to a flood of a given magnitude and shape. It would be useful to check the framework for a wider variety of catchments and events to explore whether the results obtained here can be extrapolated to other cases. The framework should be also very

useful for practical purposes in flood estimation and flood forecasting as it may assist in better understanding hydrologic systems and hydrological modelling for a range of event types.

Acknowledgments

Financial support from the EC (Project no. 037024, HYDRATE) and from the FWF Project P18993-N10 are acknowledged.

References

- Aryal, S., O'Loughlin, E., Mein, R., 2002. A similarity approach to predict landscape saturation in catchments. *Water Resources Research* 38 (10), 1208. doi:10.1029/2001WR000864.
- Atkinson, S., Sivapalan, M., Woods, R., 2002. Climate and landscape controls on water balance model complexity over changing timescales. *Water Resources Research* 38 (12), 1314. doi:10.1029/2002WR001487.
- Bergström, S., 1976. Development and application of a conceptual runoff model for Scandinavian catchments. *Bulletin Series A*, vol. 52. SMHI, Norrköping. 134 pp.
- Beven, K.J., 1979. Generalized kinematic routing method. *Water Resources Research* 15 (5), 1238–1242.
- Blöschl, G., 2006. Hydrologic synthesis: across processes, places, and scales. *Water Resources Research* 42 (3), W03S02. doi:10.1029/2005WR004319.
- Blöschl, G., Sivapalan, M., 1995. Scale issues in hydrological modeling – a review. *Hydrological Processes* 9 (3–4), 251–290. doi:10.1002/hyp.3360090305.
- Blöschl, G., Reszler, C., Komma, J., 2008. A spatially distributed flash flood forecasting model. *Environmental Modelling & Software* 23 (4), 464–478.
- Borga, M., Boscolo, P., Zanon, F., Sangati, M., 2007. Hydrometeorological analysis of the August 29, 2003 flash flood in the eastern Italian Alps. *Journal of Hydrometeorology* 8 (5), 1049–1067. doi:10.1175/JHM593.1.
- Borga, M., Gaume, E., Creutin, J.D., Marchi, L., 2008. Surveying flash floods: gauging the ungauged extremes. *Hydrological Processes* 22 (18), 3883–3885. doi:10.1002/hyp.7111.
- Chow, V.T., Maidment, D.R., Mays, L.W., 1988. *Applied Hydrology*, international ed. McGraw-Hill Book Company. pp. 572.
- Dooge, J.C., 1986. Looking for hydrologic laws. *Water Resources Research* 22 (9), 46–58.
- Farmer, D., Sivapalan, M., Jothityangkoon, C., 2003. Climate, soil, and vegetation controls upon the variability of water balance in temperate and semiarid landscapes: downward approach to water balance analysis. *Water Resources Research* 39 (2), 1035. doi:10.1029/2001WR000328.
- Fischer, H., List, E., Koh, R., Imberger, J., Brooks, N., 1979. *Mixing in Inland and Coastal Waters*. Academic Press, New York. pp. 483.
- Grayson, R.B., Blöschl, G., 2000. *Spatial Modelling of Catchment Dynamics*. Cambridge University Press, Cambridge (pp. 51–81, Chapter 3).
- Gutknecht, D., Reszler, C., Blöschl, G., 2002. Das Katastrophenhochwasser vom 7. August 2002 am Kamp – eine erste Einschätzung (The August 7, 2002 – flood of the Kamp – a first assessment). *Elektrotechnik und Informationstechnik* 119 (12), 411–413.
- Hirschboeck, K., Ely, L., Maddox, R., 2000. Hydroclimatology of meteorologic floods. In: Wohl, E. (Ed.), *Inland Flood Hazards: Human, Riparian and Aquatic Communities*. Cambridge Univ. Press, New York, pp. 39–72.
- Komma, J., Blöschl, G., Reszler, C., 2008. Soil moisture updating by ensemble kalman filtering in real-time flood forecasting. *Journal of Hydrology* 357, 228–242.
- Larsen, J., Sivapalan, M., Coles, N., Linnet, P., 1994. Similarity analysis of runoff generation processes in real-world catchments. *Water Resources Research* 30 (6), 1641–1652.
- McDonnell, J.J., Woods, R., 2004. On the need for catchment classification. *Journal of Hydrology* 299 (1–2), 2–3. doi:10.1016/j.jhydrol.2004.09.003.
- Merz, R., Blöschl, G., 2003. A process typology of regional floods. *Water Resources Research* 39 (12), 1340. doi:10.1029/2002WR001952.
- Merz, R., Blöschl, G., 2005. Flood frequency regionalisation-spatial proximity vs. catchment attributes. *Journal of Hydrology* 302 (1–4), 283–306.
- Merz, R., Blöschl, G., 2008b. Flood frequency hydrology: 2. Combining data evidence. *Water Resources Research* 44, W08433. doi:10.1029/2007WR006745.
- Merz, R., Blöschl, G., 2008a. Flood frequency hydrology: 1. Temporal, spatial, and causal expansion of information. *Water Resources Research* 44, W08432. doi:10.1029/2007WR006744.
- Mudelsee, M., Bönngen, M., Tetzlaff, G., Grünwald, U., 2004. Extreme floods in central Europe over the past 500 years: role of cyclone pathway “Zugstrasse Vb”. *Journal of Geophysical Research – Atmospheres* 109 (D23), D23101. doi:10.1029/2004JD005034.
- Norbiato, D., Borga, M., Degli, S., Esposito, E., Anquetin, Gaume S., 2008. Flash flood warning based on rainfall depth-duration thresholds and soil moisture conditions: an assessment for gauged and ungauged basins. *Journal of Hydrology* 362 (3–4), 274–290. doi:10.1016/j.jhydrol.2008.08.023.
- Parajka, J. et al., 2010. Seasonal characteristics of flood regimes across the alpine-carpathian range. *Journal of Hydrology* 394 (1–2), 78–89. doi:10.1016/j.jhydrol.2010.05.015.
- Parajka, J., Merz, R., Blöschl, G., 2005. A comparison of regionalisation methods for catchment model parameters. *Hydrology and Earth System Sciences* 9, 157–171.

- Pilgrim, D.H., 1976. Travel times and nonlinearity of flood runoff from tracer measurements on a small watershed. *Water Resources Research* 12 (3), 487–496.
- Reszler, C., Komma, J., Blöschl, G., Gutknecht, D., 2006. Ein ansatz zur identifikation flächendetaillierter abflussmodelle für die hochwasservorhersage. *Hydrologie und Wasserbewirtschaftung* 50 (5), 220–232.
- Reszler, C., Komma, J., Blöschl, G., Gutknecht, D., 2008. Dominante prozesse und ereignistypen zur plausibilisierung flächendetaillierter niederschlag-abflussmodelle. *Hydrologie und Wasserbewirtschaftung* 54 (3), 120–131 (dominant processes and event types for checking the plausibility of spatially distributed runoff models).
- Rinaldo, A., Marani, A., Rigon, R., 1991. Geomorphological dispersion. *Water Resources Research* 27 (4), 513–525.
- Robinson, J., Sivapalan, M., 1995. Catchment-scale runoff generation model by aggregation and similarity analyses. *Hydrological Processes* 9 (5–6), 555–574.
- Robinson, J., Sivapalan, M., 1997. An investigation into the physical causes of scaling and heterogeneity of regional flood frequency. *Water Resources Research* 33 (5), 1045–1059.
- Robinson, J., Sivapalan, M., Snell, J., 1995. On the relative roles of hillslope processes, channel routing, and network geomorphology in the hydrologic response of natural catchments. *Water Resources Research* 31 (12), 3089–3101.
- Rodriguez-Iturbe, I., Valdes, J., 1979. Geomorphologic structure of hydrologic response. *Water Resources Research* 15 (6), 1409–1420.
- Saulnier, G., Le Lay, M., 2009. Sensitivity of flash-flood simulations on the volume, the intensity, and the localization of rainfall in the Cévennes-Vivarais region (France). *Water Resources Research* 45, W10425. doi:10.1029/2008WR006906.
- Sivapalan, M., Beven, K.J., Wood, E.F., 1987. On hydrologic similarity. 2. A scaled model of storm runoff production. *Water Resources Research* 23 (12), 2266–2278.
- Viglione, A., Chirico, G.B., Woods, R., Blöschl, G., 2010. Generalised synthesis of space-time variability in flood response: an analytical framework. *Journal of Hydrology* 394 (1–2), 198–212. doi:10.1016/j.jhydrol.2010.05.047.
- Wagner, T., Sivapalan, M., Troch, P., Woods, R., 2007. Catchment classification and hydrologic similarity. *Geography Compass* 1 (4), 901–931. doi:10.1111/j.1749-8198.2007.00039.x.
- Wagner, W. et al., 2008. Temporal stability of soil moisture and radar backscatter observed by the advanced synthetic aperture radar (asar). *Sensors* 8 (2), 1174–1197.
- Wagner, W., Blöschl, G., Pampaloni, P., Calvet, J.-C., Bizzarri, B., Wigneron, J.-P., Kerr, Y., 2007. Operational readiness of microwave remote sensing of soil moisture for hydrologic applications. *Nordic Hydrology* 38 (1), 1–20.
- Western, A., Grayson, R.B., Blöschl, G., Willgoose, G., McMahon, T., 1999. Observed spatial organization of soil moisture and its relation to terrain indices. *Water Resources Research* 35 (3), 797–810.
- Wood, E.F., Hebson, C.S., 1986. On hydrologic similarity. 1. Derivation of the dimensionless flood frequency curve. *Water Resources Research* 22 (11), 1549–1554.
- Woods, R., 1997. A search for fundamental scales in runoff generation: combined field and modelling approach. Ph.D. thesis, Dept. of Environmental Engineering, University of Western Australia, Nedlans, Western Australia.
- Woods, R., Sivapalan, M., 1999. A synthesis of space-time variability in storm response: rainfall, runoff generation, and routing. *Water Resources Research* 35 (8), 2469–2485.
- Woods, R., Grayson, R.B., Western, A., Duncan, M., Wilson, D., Young, R., Ibbitt, R., Henderson, R., McMahon, T., 2001. Experimental design and initial results from the Mahurangi River variability experiment: MARVEX. In: Lakshmi, V., Albertson, J., Schaake, J.C.J. (Eds.), *Observations and Modeling of Land Surface Hydrological Processes*, Water Resources Monograph, vol. 3. American Geophysical Union, pp. 201–Washington, DC.
- Zoccatelli, D., Borga, M., Zanon, F., Antonescu, B., Stancalie, G., this issue, Which rainfall spatial information for flash flood response modelling? A numerical investigation based on data from the Carpathian range, Romania. *Journal of Hydrology*.